Article

Neuron

Dysregulated ADAM10-Mediated Processing of APP during a Critical Time Window Leads to Synaptic Deficits in Fragile X Syndrome

Highlights

- FMRP regulates APP synthesis and cleavage during mouse synaptogenesis
- APP-ADAM10 pathway is dysregulated in Fragile X patients
- Excess of sAPPα increases immature spines, mRNA translation, and mGluR-mediated LTD
- Targeting the APP-ADAM10 pathway could be beneficial to FXS

Authors

Emanuela Pasciuto, Tariq Ahmed, Tina Wahle, ..., Monica Di Luca, Bart De Strooper, Claudia Bagni

Correspondence

claudia.bagni@cme.vib-kuleuven.be

In Brief

Pasciuto et al. show that dual dysregulation of APP and ADAM10, during a critical period of postnatal development, leads to overproduction of sAPPα. Modulation of ADAM10 activity re-establishes physiological sAPPα levels and ultimately ameliorates FXS molecular, synaptic, and behavioral deficits.

Pasciuto et al., 2015, Neuron *87*, 382–398
July 15, 2015
http://dx.doi.org/10.1016/j.neuron.2015.06.032

CellPress

CellPress

Neuron
Article

Dysregulated ADAM10-Mediated Processing of APP during a Critical Time Window Leads to Synaptic Deficits in Fragile X Syndrome

Emanuela Pasciuto,[1,2] Tariq Ahmed,[3] Tina Wahle,[1,2] Fabrizio Gardoni,[4] Laura D'Andrea,[5] Laura Pacini,[5] Sébastien Jacquemont,[6,7,8] Flora Tassone,[9,10] Detlef Balschun,[3] Carlos G. Dotti,[1,2,11] Zsuzsanna Callaerts-Vegh,[3] Rudi D'Hooge,[3] Ulrike C. Müller,[12] Monica Di Luca,[4] Bart De Strooper,[1,2,13] and Claudia Bagni[1,2,5,*]

[1]Center for Human Genetics and Leuven Research Institute for Neuroscience and Disease (LIND), KU Leuven, 3000 Leuven, Belgium
[2]VIB Center for the Biology of Disease, 3000 Leuven, Belgium
[3]Faculty of Psychology and Educational Sciences, Laboratory of Biological Psychology, KU Leuven, 3000 Leuven, Belgium
[4]Dipartimento di Scienze Farmacologiche e Biomolecolari and Centre of Excellence on Neurodegenerative Diseases, Università degli Studi di Milano, 20133 Milan, Italy
[5]Department of Biomedicine and Prevention, University of Rome Tor Vergata, 00133 Rome, Italy
[6]Service de Génétique Médicale, Centre Hospitalier Universitaire Vaudois, 1011 Lausanne, Switzerland
[7]Department of Psychiatry, University of Montreal, QC H3T 1C5, Canada
[8]Centre de Recherche, Centre Hospitalier Universitaire Sainte Justine, Montréal, QC H3T 1C4, Canada
[9]Department of Biochemistry and Molecular Medicine, UC Davis, Sacramento, CA 95817, USA
[10]MIND Institute, UC Davis Medical Center, Sacramento, CA 95817, USA
[11]Centro de Biología Molecular Severo Ochoa, CSIC/UAM, 28049 Madrid, Spain
[12]Institute for Pharmacy and Molecular Biotechnology, University of Heidelberg, 69120 Heidelberg, Germany
[13]UCL Institute of Neurology, Queen Square, WC1N 3BG London, UK
*Correspondence: claudia.bagni@cme.vib-kuleuven.be
http://dx.doi.org/10.1016/j.neuron.2015.06.032

SUMMARY

The Fragile X mental retardation protein (FMRP) regulates neuronal RNA metabolism, and its absence or mutations leads to the Fragile X syndrome (FXS). The β-amyloid precursor protein (APP) is involved in Alzheimer's disease, plays a role in synapse formation, and is upregulated in intellectual disabilities. Here, we show that during mouse synaptogenesis and in human FXS fibroblasts, a dual dysregulation of APP and the α-secretase ADAM10 leads to the production of an excess of soluble APPα (sAPPα). In FXS, sAPPα signals through the metabotropic receptor that, activating the MAP kinase pathway, leads to synaptic and behavioral deficits. Modulation of ADAM10 activity in FXS reduces sAPPα levels, restoring translational control, synaptic morphology, and behavioral plasticity. Thus, proper control of ADAM10-mediated APP processing during a specific developmental postnatal stage is crucial for healthy spine formation and function(s). Downregulation of ADAM10 activity at synapses may be an effective strategy for ameliorating FXS phenotypes.

INTRODUCTION

Brain development is a life-long project. While it is well accepted that the brain undergoes critical periods in its development, the molecular basis of these critical periods is not fully understood. The events that shape the brain during development influence processing of new information, acquisition of new skills, and formation of memories throughout life. Proper synaptic contacts, trans synaptic signaling, and structural remodeling are essential aspects of synapse maturation and stabilization during postnatal brain development (Grant, 2012; Yuste, 2013). Fine-tuned expression of several proteins is fundamental for the synaptic structure, the establishment of synaptic networks, and neuronal plasticity (Sala and Segal, 2014). Changes in dendritic spine morphology and plasticity are associated with various neurodevelopmental diseases, such as Down syndrome, Rett syndrome, autism spectrum disorder (ASD), and Fragile X syndrome (FXS) (Sala and Segal, 2014).

FXS is the most common form of inherited intellectual disability and about 30% of FXS children meet the criteria for ASD (Jacquemont et al., 2007; Lozano et al., 2014). Patients with FXS have cognitive and behavioral deficits, anxiety, and a susceptibility to epilepsy (Jacquemont et al., 2007; Lozano et al., 2014). At the cellular level, FXS neurons have an increased number of dendritic spines that appear long, thin, and tortuous (Hinton et al., 1991; Irwin et al., 2001). The mouse model of FXS (*Fmr1* knockout [KO]) exhibits morphological, synaptic, and behavioral alterations similar to human patients (Bakker, 1994; Comery et al., 1997; Huber et al., 2002; Santos et al., 2014).

FXS is due to the absence of, or mutations in, the Fragile X mental retardation protein, FMRP, an RNA-binding protein. Through four RNA-binding domains, FMRP associates with messenger RNAs (mRNAs) encoding pre- and postsynaptic proteins and regulates multiple steps of mRNA metabolism, such as dendritic transport, stability, and translation (Darnell and Klann,

2013; Pasciuto and Bagni, 2014a, 2014b). Loss of FMRP compromises the fine-tuned expression of a variety of proteins, leading to deficits in embryonic and early postnatal brain wiring networks (La Fata et al., 2014; Romano et al., 2014). Mutations in several of the FMRP target mRNAs are associated with different forms of intellectual disability such as ASD, mood disorders, and schizophrenia (Pasciuto and Bagni, 2014b). A mechanism through which FMRP inhibits translation of synaptic mRNAs is via the cytoplasmic FMRP interacting protein 1 (CYFIP1) that acts as an eIF4E-binding protein (De Rubeis et al., 2013; Genheden et al., 2015; Napoli et al., 2008; Panja et al., 2014). Among the bona-fide mRNAs regulated by FMRP (Pasciuto and Bagni, 2014b) is the transcript encoding the amyloid precursor protein (APP) (Napoli et al., 2008; Westmark and Malter, 2007). APP is a type I transmembrane protein that plays a central role in Alzheimer's disease (AD) (Rajendran and Annaert, 2012) and is also dysregulated in neurodevelopmental disorders, such as Down syndrome (Glenner and Wong, 1984), FXS, and ASD (Ray et al., 2011; Westmark et al., 2011). APP was initially described as a cell-surface receptor (Kang et al., 1987) that interacts with a variety of molecules and some components of the extracellular matrix (Reinhard et al., 2013), thus activating transmembrane signal transduction, calcium metabolism, and/or transcription (Müller and Zheng, 2012; Rice et al., 2013). A wide range of APP functions have been described in both the developing and adult brain, including neurite outgrowth, synaptic development and plasticity, cell adhesion, protein trafficking, and cell migration (Hoe et al., 2012; Müller and Zheng, 2012). Consistent with its functions, APP expression is high during spine formation and progressively declines after synaptic maturation (Moya et al., 1994). Alterations of synaptic structure and function are therefore well established features of APP dysregulation, although the underlying complex molecular mechanism(s) are poorly understood.

While impaired learning and memory and reduced long-term plasticity have been consistently found in aged *App* KO mice (Ring et al., 2007; Tyan et al., 2012), the effects of APP deletion on dendritic spine density are quite controversial (Hoe et al., 2012). Both increased (Bittner et al., 2009) and reduced mature spine density (Lee et al., 2010b; Tyan et al., 2012) have been reported in the cortex of APP-deficient mice. Overexpression of APP consistently increases spine number and promotes synaptogenesis (Lee et al., 2010b).

On the cell surface, APP processing generates a secreted form of APP (sAPPα) and a C-terminal fragment (CTFα). Soluble APPα is upregulated during synaptogenesis and increases synaptic density, cortical synaptogenesis, and memory retention in vivo (Bell et al., 2008; Hick et al., 2015; Roch et al., 1994; Tyan et al., 2012), and it has been proposed to have both a neurotrophic and neuroprotective effect (Milosch et al., 2014; Müller and Zheng, 2012). The disintegrin metalloprotease ADAM10 is the constitutive α-secretase required for sAPPα generation (Kuhn et al., 2010). Its function is essential for cortex formation and for spine morphology (Jorissen et al., 2010; Malinverno et al., 2010). ADAM10 overexpression promotes cortical synaptogenesis (Bell et al., 2008), whereas its depletion causes synaptic defects and impaired learning (Prox et al., 2013). A different APP processing pathway, mediated by the β-secretase BACE1, cleaves APP, generating a soluble form of APP (sAPPβ) and a C-terminal membrane-associated fragment (CTFβ). The formation of β-amyloid (Aβ40-42) in the brain is critical for AD progression (Karran et al., 2011; Selkoe, 2002).

Here, we highlight the critical role played by FMRP in coordinating the production of sAPPα in the brain. Soluble APPα accumulates in the FXS brain as a result of excessive synthesis of APP and ADAM10 proteins during a critical postnatal period. The excess of generated sAPPα drives an increase in protein synthesis, formation of immature spines, and impaired synaptic plasticity. This cascade of events requires the metabotropic glutamate receptor 5 signaling and activates the mitogen-activated protein kinase (MAPK) pathway. Finally, we show that modulation of ADAM10 activity at FXS synapses ameliorates various molecular, synaptic, and behavioral defects in FXS.

RESULTS

FMRP Regulates APP Protein Processing at Early Postnatal Stages

The levels of APP are increased when FMRP is absent (Westmark and Malter, 2007) or when CYFIP1 levels are decreased in juvenile mice (Napoli et al., 2008). Because FXS is a neurodevelopmental disorder, we characterized the changes of APP expression during brain development in the *Fmr1* KO mouse model (Bakker, 1994). Whole brain extracts from wild-type (WT) and *Fmr1* KO mice were analyzed during early postnatal stages (P7, P14, and P21) and adulthood (P30 and P90). No differences in APP expression were observed between WT and KO mice at P7 and P14, whereas a significant upregulation was observed in the *Fmr1* KO mice starting at 3 weeks after birth (P21) and was maintained throughout adulthood (Figure 1A). A similar dysregulation was observed at synapses (Figure 1B). *App* mRNA steady-state levels were not changed in the absence of FMRP (Figure S1A).

Therefore, absence of FMRP leads to increased APP expression in the brain during a period critical for the stabilization of synapses and development of brain functions (Grant, 2012; Yuste, 2013).

It has been hypothesized that the excess of APP in FXS might be pathogenic due to elevated Aβ release (Westmark and Malter, 2007). We measured Aβ levels in cortex during synaptogenesis and in adulthood. Unexpectedly, we observed a significant decrease in Aβ in juvenile *Fmr1* KO mice compared to WT (Figure 2A). Only at the adult stage are Aβ levels increased (Figure 2A). We next analyzed the production of secreted sAPP and CTFs using specific antibodies (Figures S2A, S4B, and S4C). Brains were fractionated (Figure S2B) and the levels of sAPP (total sAPP, sAPPα, and sAPPβ) quantified. Absence of FMRP leads to a parallel increase of APP and sAPP protein levels between the third and fifth postnatal week (P21–P30) (Figures 1A and 2B). Specifically, we found a rise in sAPPα levels in juvenile (P21) *Fmr1* KO mice and a decrease in β-cleavage (less sAPPβ; Figure 2C). We next investigated APP processing at FXS synapses by measuring the CTFs generated in the synaptic membrane. Using an established biochemical synaptosome

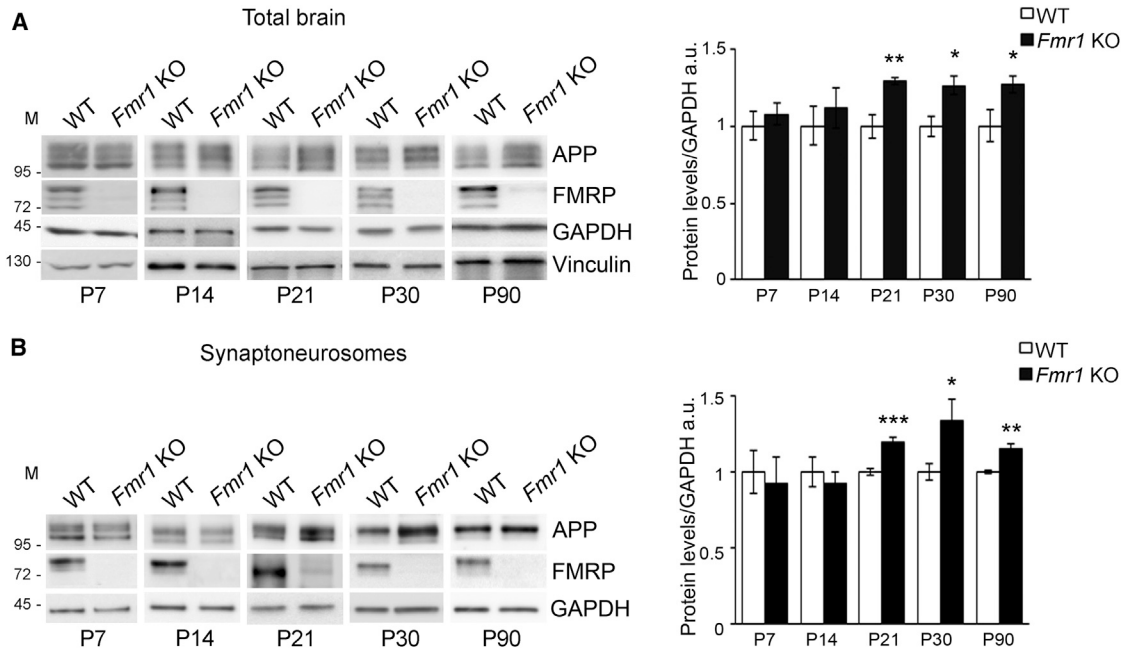

Figure 1. FMRP Regulates APP Protein Level during Postnatal Development

(A) In *Fmr1* KO mice, APP protein levels are upregulated during brain development. The protein expression was analyzed during development by WB in WT and KO mouse brain. For APP antibody specificity see Figures S2, S4, and S6B. Representative western blot showing protein levels at P7, P14, P21, P30, and P90. The histograms show quantified protein levels normalized to glyceraldehyde 3-phosphate dehydrogenase (GAPDH). This ratio was set to 1 in the WT mice for each developmental stage. The bars represent the SEM (*$p < 0.05$; **$p < 0.01$, Student's t test) (n = 4 for each developmental stage).

(B) APP levels are increased in *Fmr1* KO synaptoneurosomes. Representative western blot showing protein levels at P7, P14, P21, P30, and P90 in WT and *Fmr1* KO mice. The histograms show quantified APP expression normalized to GAPDH. This ratio in WT mice was set to 1. The bars represent the SEM (*$p < 0.05$; **$p < 0.01$, ***$p < 0.001$, Student's t test) (n = 3–4).

See also Figure S1.

fractionation (Galli et al., 1996; Marcello et al., 2007), we isolated detergent resistant membrane from synaptoneurosomes (DRM; Figure S2C). These samples are enriched in membrane-associated proteins, such as Synaptophysin, PSD95, Flotillin, and NMDA receptor subunits. We found that APP protein levels were less abundant in the synaptic membranes isolated from *Fmr1* KO (Figure 2D). In the absence of FMRP, the levels of CTFα (~10 kDa) generated by α-secretase activity were increased, whereas CTFβ (~12 kDa), the β-secretase product, was decreased (Figure 2D). The altered CTFα/CTFβ ratio suggests that α-secretase activity is specifically upregulated in juvenile *Fmr1* KO animals. Because α- and β-secretases compete to cleave APP, the observed reduction of sAPPβ, CTFβ, and Aβ supports a skewed APP processing toward the non-amyloidogenic pathway in the *Fmr1* KO during early stages of development and a possible switch toward the β-cleavage at later stages.

Absence of FMRP Reduces Cell-Surface APP Protein Levels

The concomitant increase in sAPPα and decrease of sAPPβ protein levels in the *Fmr1* KO suggested that APP was highly processed at the cell surface. First, we determined total and surface APP levels in cortical neurons from WT and KO mice by immunofluorescence (Figure 2E). Total APP levels were detected by an antibody against the cytoplasmic domain (A8717; Figures S2A and S2B) and the surface level of APP using an antibody against its ectodomain (22C11; Figures S2A and S2B). Total APP levels were higher in *Fmr1* KO than in WT cortical neurons, as in brain extracts, but the surface APP was lower in the FMRP-deficient cells (Figure 2E). To corroborate our data, we biotinylated and captured cell-surface proteins and analyzed the precipitate by western blotting (WB) (Figure 2F). Although the total APP expression was increased in *Fmr1* KO mice, the surface APP was decreased. Both experiments showed that, in FMRP-deficient neurons, the global expression of APP is increased; however, there is a steep decrease in full-length APP protein levels at the cell surface (Figures 2E and 2F). While we cannot rule out that a defect in APP trafficking could also contribute to the reduced APP present at the cell surface, the decrease in surface APP and the parallel increase in sAPP released in the media of *Fmr1* KO neurons (Figure 2G) strongly support that APP processing at the membrane is upregulated.

ADAM10 Protein Levels Are Upregulated in the Absence of FMRP

To identify the mechanisms underlying the decreased APP at the cell surface and the increased sAPPα release in FXS, we measured the expression levels of the constitutive APP

α-secretase ADAM10 (Jorissen et al., 2010). WB of cortical (Figure 3A) and synaptic lysates (Figure 3B) showed a parallel increase in the expression of APP and mature ADAM10 in the absence of FMRP, while the synaptic expression of two other metalloproteases ADAM9 and 17 did not change (Figure 3B). Furthermore, the absence of FMRP leads to a developmental stage-specific increase of ADAM10 (Figure 3C), correlating with the increased production of sAPPα between the third and fourth postnatal week (Figure 2B). The increase of ADAM10 in *Fmr1* KO cortical neurons was confirmed by immunofluorescence (Figure 3D). Opposite distribution to APP was observed for the mature ADAM10 protein, which was increased at the cell-surface (Figure 3E), where it cleaves APP to generate sAPPα (Lichtenthaler, 2011). The increased ADAM10 expression in the *Fmr1* KO mice, at this specific developmental stage, did not result in a dysregulation of other protein targets such as Notch and N-cadherin (Figure S3).

Overall, these observations support the conclusion that FMRP, by coordinating both APP and ADAM10 expression, specifically regulates sAPPα generation during the critical period of synaptogenesis.

FMRP Regulates the ADAM10-APP Pathway at the Level of mRNA Translation

To test whether FMRP is directly involved in the generation of excessive levels of sAPPα, we investigated if FMRP directly regulates *App* and *Adam10* mRNA metabolism in juvenile mice. FMRP was immunoprecipitated (IP) from brain extracts, and the bound mRNAs were analyzed by RT-PCR. *App* and *Adam10* mRNAs were both associated with FMRP. The specificity of this interaction was confirmed by the absence of *Adam9* and *Adam17* mRNAs and the non-target *D2DR* and *Cyp46* mRNAs (Figure 3F). *App* and *Adam10* mRNA steady-state levels did not significantly change between WT and *Fmr1* KO cortices (Figure S1B). Therefore, we assessed whether FMRP controls APP and ADAM10 protein synthesis. The mouse cortex was fractionated in translationally active polysomes and silent mRNPs and the mRNA distribution was analyzed as previously described (Zalfa et al., 2007). As shown in Figure 3G, *App* and *Adam10* mRNAs co-fractionated with the polysomal fraction more in the *Fmr1* KO brain than in WT; in contrast, the levels of *β-actin* mRNA were unchanged, consistent with previous findings (Lee et al., 2010a).

Our data indicate that FMRP regulates *App* and *Adam10* mRNA translation. In the FXS mouse model, the lack of FMRP-mediated translational repression increases APP and ADAM10 protein levels and ultimately generates the excess of sAPPα.

sAPPα Contributes to the FXS Spine Phenotype

To address the contribution of excessive APP synthesis and processing to the spine dysgenesis observed in FXS, we reduced APP in *Fmr1* KO neurons (DIV 8), a stage in which neurons are still immature and APP is not dysregulated (Figure S4A). We knocked down APP using a lentiviral vector (Lee et al., 2010b) carrying a short hairpin RNA directed specifically against *App* mRNA (*App* short hairpin [sh]RNA-EGFP; Figures S4B and S4C). Mean spine head and length measurements were used to categorize the spines into the following classes: mushroom and stubby (mature); long thin and filopodia (immature) (Harris et al., 1992) (Figure S5A). Reduction of APP in WT neurons reduced spine density, while exogenous sAPPα increased the number of immature spines (Figures S5B and S5C). The spine number and distribution along the four morphological classes significantly differed between WT and KO neurons, with the latter showing more immature spines (Figures 4 and S5C). Importantly, when sAPPα was added to the medium of WT and *Fmr1* KO neurons, in *Fmr1* KO neurons, the APP-dependent rescue of the spine density was abolished and the density of long thin spines and filopodia increased (Figures 4A–4C), resulting in an increased number of immature spines (Figures 4C and S5C). In conclusion, these data support the hypothesis that concomitant deregulation of both APP expression and processing during the early stages of development contributes to immature spine formation in FMRP-deficient neurons. Of note, similar effects have been recently observed in ADAM10 heterozygous mice (Prox et al., 2013), further supporting that the dual-level APP-ADAM10 is necessary for proper spine development and density.

Excessive ADAM10 Activity Causes Exaggerated Protein Synthesis in the *Fmr1* KO Mice

FXS mice have exaggerated protein synthesis (Bagni et al., 2012). To explore whether sAPPα promotes protein synthesis in FXS, we used the SUnSET technology, a non-radioactive assay for labeling newly synthesized proteins (Schmidt et al., 2009) (Figure S6A). The level of protein synthesis was monitored in cortical neurons and synaptoneurosomes from WT, *Fmr1* KO, and *Fmr1* KO/*App* heterozygous (Het) mice (Figures 5A and 5B) and in both cases protein synthesis was elevated in the absence of FMRP. Genetic reduction of APP in *Fmr1* KO/App^{Het} mice returned the protein synthesis rate to WT level (Figure 5A). *App* KO mice also showed a reduced protein synthesis at synapses, further supporting a role for APP in the regulation of translation in neurons (Figure S6B). Furthermore, treatment of WT and *Fmr1* KO/*App*^{Het} neurons with sAPPα led to an increase in protein synthesis (Figures 5C and 5D). Treatment of WT neurons with sAPPβ did not elicit protein synthesis (data not shown). To finally relate the sAPPα-dependent increase in protein synthesis to the excessive ADAM10 activity, we crossed the *Fmr1* KO with the *Adam10*^{Het} mice and monitored basal protein synthesis at synapses. Genetic reduction of ADAM10 also lowered the rate of de novo protein synthesis in the *Fmr1* KO (Figure 5E). Similarly, absence of ADAM10 in mouse embryonic fibroblasts (Figure S6C) and haploinsufficiency of ADAM10 in cortical neurons (Figure S6D) decreases protein synthesis.

Taken together, these findings show that FXS mice have aberrant sAPPα-dependent de novo protein synthesis.

sAPPα Promotes Metabotropic Glutamate Receptor 5 Signaling

Metabotropic glutamate receptor 5 (mGluR5) and MAPK signaling are affected in FXS (Osterweil et al., 2010). To investigate a possible crosstalk between sAPPα-mediated increase in protein synthesis and mGluR5 activation, we treated cortical neurons with sAPPα and monitored the activation of the MAPK

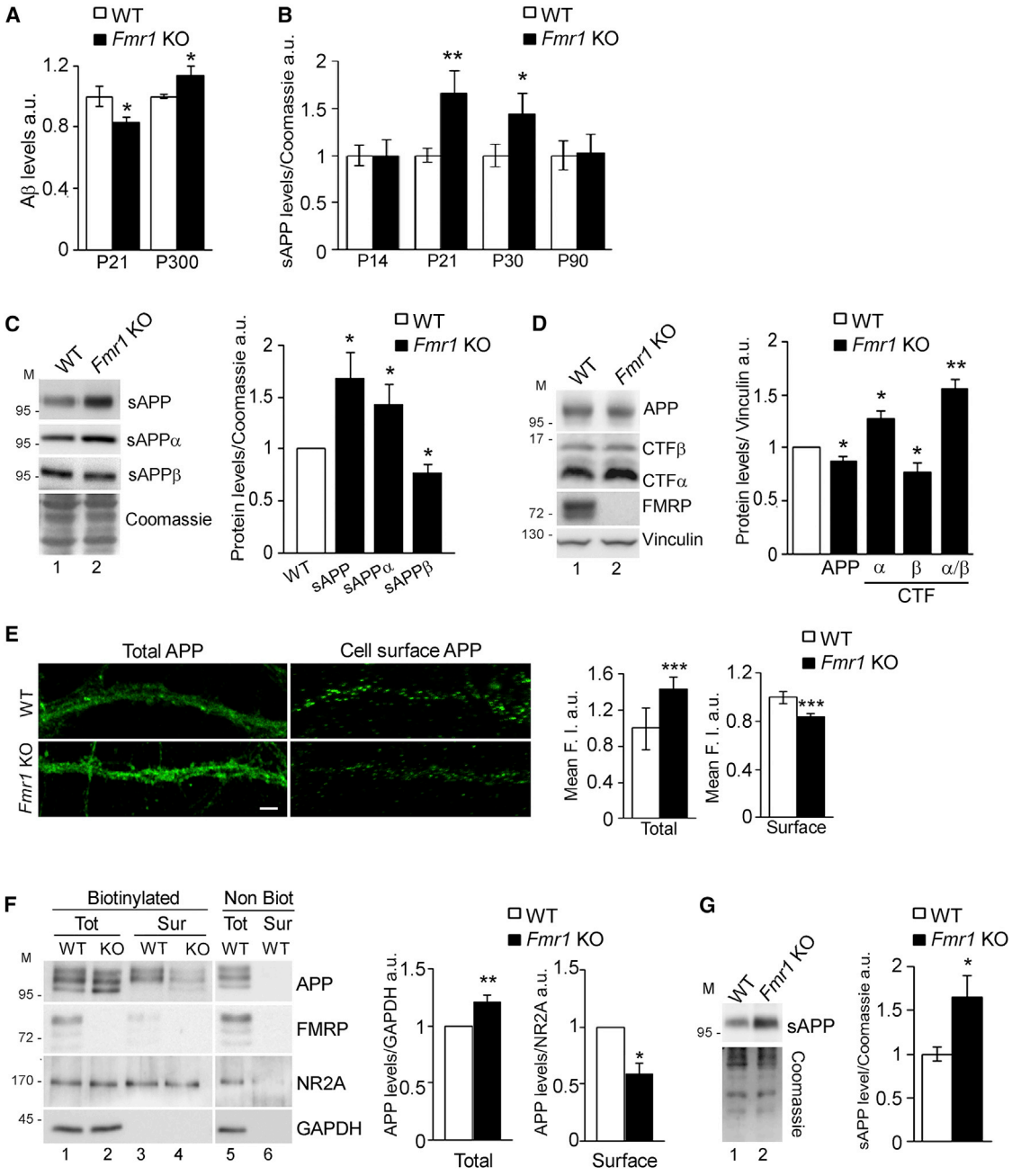

Figure 2. Impaired Processing of APP in *Fmr1* KO Mice Leads to Enhanced sAPPα Release

(A) Aβ40 levels in juvenile and aged *Fmr1* KO cortices. The amount of Aβ was measured by ELISA normalized to the brain's weight and expressed as the percentage of the WT. The bars represent the SEM (*p < 0.05, Student's t test) (n = 4 for both P21 and P300).

(B) sAPP levels in KO brain cortices during postnatal development. The histograms show the quantification of sAPP protein levels normalized to Coomassie. The bars represent the SEM (*p < 0.05, **p < 0.01, Student's t test) (n = 3).

(C) APP processing in P21 KO brain cortices. Representative WB showing protein levels of sAPP (sAPPα + sAPPβ), sAPPα, and sAPPβ in the soluble fraction (see also Figure S2) in WT and KO cortices. The histograms show the quantification of the three products normalized to Coomassie. The bars represent the SEM (*p < 0.05, one-sample t test) (n = 4).

(D) α- and β-secretase products in WT and *Fmr1* KO synaptic membranes. APP, APP CTFα (~10 kDa) and CTFβ (~12 kDa), FMRP, and Vinculin protein levels were analyzed by WB in the synaptic membranes of WT and KO mice. The histograms show quantified proteins normalized to Vinculin. This ratio in WT mice was set to 1. The bars represent the SEM (*p < 0.05, **p < 0.01, one-sample t test) (n = 6). See also Figure S2.

(E) Cell-surface APP is reduced in *Fmr1* KO cortical neurons. The WT and KO cortical neurons were stained for total APP (left) or surface APP (right). The representative dendritic fragments (>50 μm distance from the cell body) are shown. The histograms show the total and surface protein levels as the mean fluorescence intensity (Mean F.I.). The bars represent SEM (***p < 0.001, Student's t test) (n = 8 cells, five dendritic fragments [20 μm/cell]). The scale bar corresponds to 5 μm.

(legend continued on next page)

signaling cascade downstream of mGluR5. Soluble APPα induced an increase in phosphorylated extracellular signal-regulated kinase (ERK) 1/2 (Figure 5F). This was mediated via the activation of the mGluR1/5 receptor, because its effect was abolished by the mGluR5 antagonist MPEP (Figure 5F). Rapamycin treatment, affecting mTOR and ERK phosphorylation in opposite directions, was used as control (Ma and Blenis, 2009). Interestingly, no effect on mTOR phosphorylation was observed upon sAPPα treatment or mGluR5 inhibition, suggesting that the mTOR pathway is not activated by sAPPα (Figure 5F).

Altogether, our data demonstrate that excessive production of sAPPα sustains the increase in mGluR-dependent protein synthesis observed in FXS, possibly through the MAPK signaling pathway.

TAT-Pro ADAM10$^{709–729}$ Peptide Normalizes Enhanced Hippocampal mGluR-Long Term Depression, Memory, and Hyperactivity in *Fmr1* KO Mice

We next examined whether lowering ADAM10 activity in *Fmr1* KO neurons might ameliorate these aberrant phenotypes. To this end, we used a cell-permeable peptide TAT-Pro ADAM10$^{709–729}$, which contains part of the intracellular domain of ADAM10; it interferes with the interaction of ADAM10 and synapse-associated protein 97 (SAP97), thereby reducing the localization and activity of ADAM10 specifically at the synapses (Marcello et al., 2007). The treatment of WT and *Fmr1* KO cortical neurons with TAT-Pro peptide reduced sAPPα release (Figure 6A). Consistently, we also reduced sAPP production in *Fmr1* KO neurons using the tissue inhibitor of metalloproteinases (TIMP-1) (Amour et al., 2000) (Figure S7A). Furthermore, a treatment of the *Fmr1* KO neurons with the TAT-Pro peptide increased the ratio of surface versus total APP levels (Figure S7B).

We next examined APP processing in juvenile (P21) WT and *Fmr1* KO mice after intraperitoneal injection of the TAT-Pro peptide (Figure 6B). Importantly, the excessive sAPPα production in the *Fmr1* KO mice, monitored by WB 18 hr after peptide injection, was no longer observed upon treatment with the peptide (Figure 6B), suggesting that the excess is produced at FXS synapses; a control peptide (TAT-Ala) had no effect.

Because one of the hallmarks of FXS is the enhanced mGluR-dependent long-term depression (LTD) observed in *Fmr1* KO mice (Huber et al., 2002), and ADAM10 activity affects LTD (Musardo et al., 2013; Prox et al., 2013), we examined whether the reduction of ADAM10 activity could ameliorate the mGluR-LTD responses in *Fmr1* KO mice. The effects of the TAT-Pro peptide on (RS)-3,5-Dihydroxyphenylglycine (DHPG) induced LTD were tested in juvenile (P18–25) WT and KO mice. Field excitatory postsynaptic potentials (fEPSPs) were recorded from CA1 neurons in hippocampal slices in response to Schaffer collateral fiber stimulation 18 hr after treatment. A bath application of DHPG (30 μM, 15 min) induced a robust LTD of fEPSPs in the WT slices (240 min: 53% ± 9% of baseline, n = 7). In agreement with previous reports (Nosyreva and Huber, 2005), we observed an enhanced DHPG-induced LTD in the *Fmr1* KO mice (240 min: 28% ± 3%, n = 12) (Figure 6C). Exposure to TAT-Pro or TAT-Ala peptides had no detectable effect on the ability of DHPG to elicit LTD in the WT slices (65% ± 8%, n = 7 and 56% ± 5%, n = 6, respectively) when compared with the untreated control (Figure 6D). These data correlate with lack of reduction of sAPPα levels upon TAT-Pro treatment in WT (Figure 6B). In contrast, we found that treatment with the TAT-Pro peptide was sufficient to prevent the enhanced LTD in the *Fmr1* KO mice, indicating that the exaggerated late LTD (>2 hr) in these mice (Figure 6E) is a direct consequence of increased ADAM10 activity. Peptide treatment did not affect basal transmission (Figures S8A and S8B).

To further address whether targeting ADAM10 could rescue the increased protein synthesis in FXS, WT and *Fmr1* KO animals were treated in vivo with the TAT-Pro peptide. FMRP targets, such as APP, ADAM10, as well as the activity-regulated cytoskeleton-associated protein (ARC) and the striatal-enriched protein tyrosine phosphatase (STEP) (Bagni et al., 2012) were detected in synaptoneurosomes of treated animals (Figure 6F). We observed that upon injection of the TAT-Pro peptide, the excessive levels of APP, ADAM10, ARC, and STEP are restored to normality. These findings are consistent with the reduction of protein synthesis observed at the synapses of the *Fmr1* KO/*Adam10*^{Het} and *Fmr1* KO/*App*^{Het} mice (Figures 5B and 5E). Finally, we monitored the effect of the peptide on working memory (T-maze) and hyperactivity (open field) (Figures 6G and 6H), two behavioral features that have been consistently found altered in FXS mice (Santos et al., 2014). *Fmr1* KO mice move faster and travel a longer distance in the open field, and they fail more in the spontaneous alternation in the T-maze (Santos et al., 2014). Nest building is a social behavior in mice impaired in Fragile X and other models of autism (Udagawa et al., 2013). *Fmr1* KO mice used less material in nest construction compared to WT animals (Figure 6I). Targeting ADAM10 trafficking with the TAT-Pro peptide ameliorates the above-mentioned behavioral deficits (Figures 6G–6I).

Together, these results demonstrate that blocking SAP97-mediated ADAM10 trafficking to the synapses reduces sAPPα production and reverses molecular, cellular, and behavioral impairments that constitute the hallmarks of FXS.

FMRP Regulated APP and ADAM10 Protein Levels in Humans

To address the relevance of our findings for the human disease, APP and ADAM10 levels were analyzed in human samples. We observed that APP is expressed at higher levels in lymphoblastoid cell lines from patients with FXS compared to controls (Figure 7A). In addition, the analysis of elderly human

(F) Surface APP is decreased in the *Fmr1* KO cortical neurons. Proteins were biotinylated and captured with streptavidin-beads (input 1/10, lanes 1, 2 and 5; surface "sur" lanes 3, 4, and 6). APP, GAPDH, NR2A, and FMRP levels were analyzed by WB. The histograms show the quantification. The changes of total versus surface APP are expressed as ratio of the WT. The bars represent the SEM (*p < 0.05, **p < 0.01, one-sample t test) (n = 4).

(G) sAPP levels are increased in cortical neurons. sAPP levels were analyzed by WB in the conditioned medium from WT and KO cortical neurons. The histograms show the quantification of APP protein levels normalized to the Coomassie. This ratio was set to 1 in the WT mice. The bars represent the SEM (*p < 0.05, Student's t test) (n = 4).

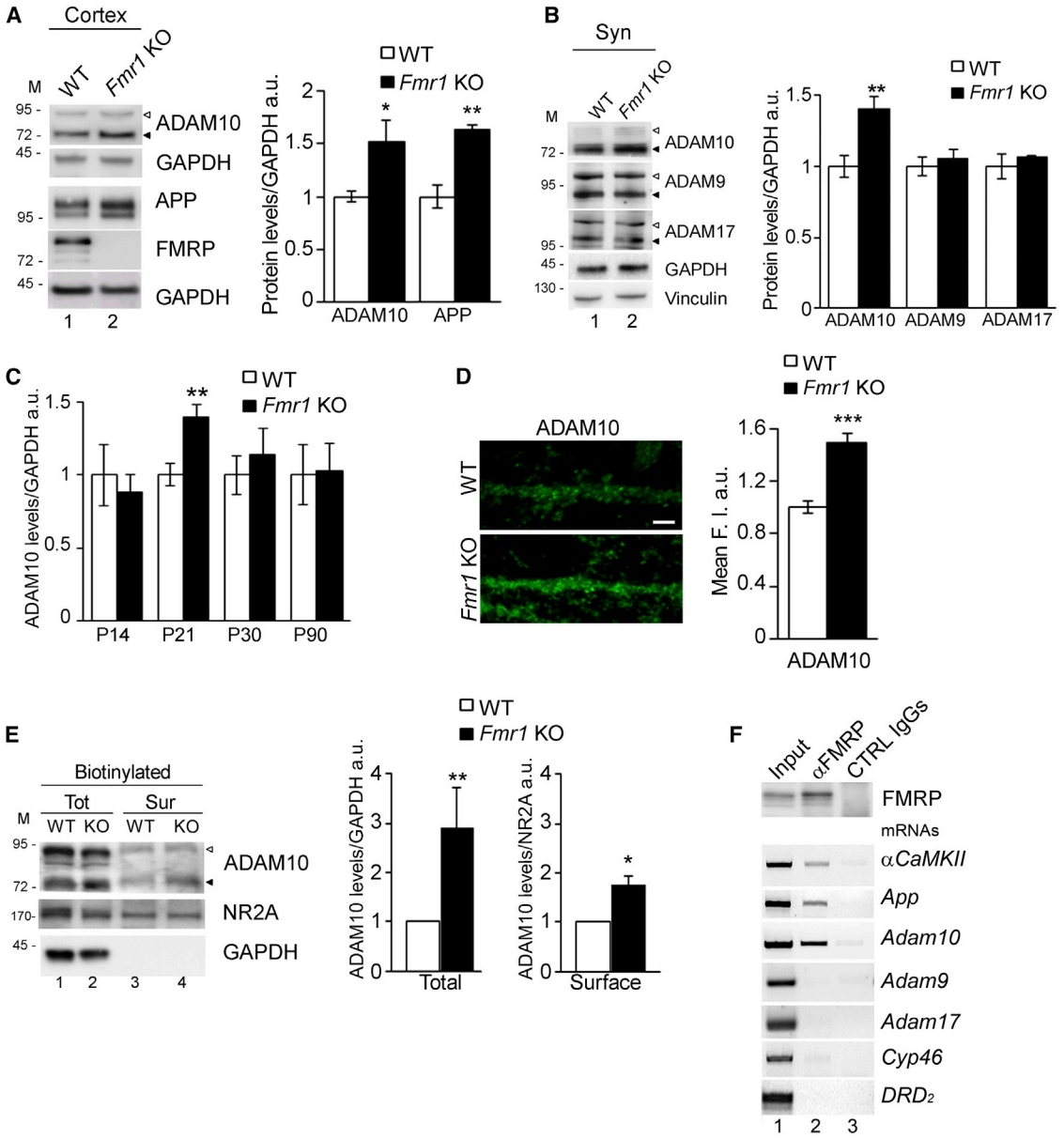

(legend on next page)

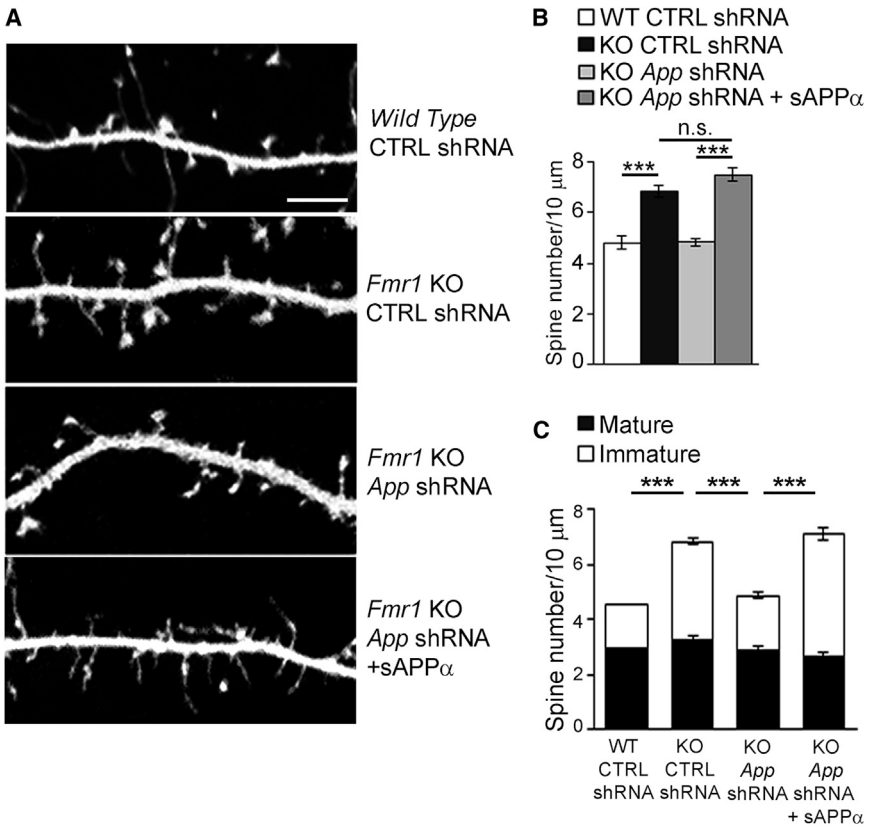

Figure 4. sAPPα Levels Are Crucial for Spine Morphology in FXS

(A) Representative dendritic segments of cultured cortical neurons transfected with lentiviral vectors expressing EGFP-*App* shRNA or EGFP-CTRL shRNA, treated with sAPPα at DIV8, and analyzed at DIV14. The scale bar represents 5 μm.

(B) Spine density of the different spine types. The bars represent the SEM (***p < 0.001, non-significant = n.s., one-way ANOVA followed by post hoc Bonferroni correction) (n = 10 neurons from at least two different cultures). For each condition, 350–500 spines were analyzed.

(C) Density of the mature and immature spines. The spine morphology was used to discriminate the spine types. See Figure S5. The bars represent the SEM (***p < 0.001, one-way ANOVA followed by post hoc Bonferroni correction) (n = 10 neurons from at least two different cultures). For each condition, 350–500 spines were analyzed.

See also Figures S4 and S5.

postmortem brains from FXS and control individuals revealed that a reduction in the levels of FMRP alters APP expression in the cortex (Figure 7B; Table S1) and cerebellum (data not shown). *APP* mRNA levels did not change significantly (Figures S1C and S1D). The dysregulation of APP protein levels are consistent with our observation in adult *Fmr1* KO brains (Figure 1). No significant changes were detected in ADAM10 levels in human postmortem brains (average age of 60) or immortalized lymphoblastoid cells from FXS compared to control individuals. These findings are consistent to what we observed in the mouse model where a development specific dysregulation of ADAM10 was observed in juvenile mice only (Figure 3C). Because human postmortem brains from adolescent FXS were not available, we analyzed APP and ADAM10 expression in primary fibroblasts obtained from adolescent and adult patients with FXS. Importantly, in these cells, APP and ADAM10 were both upregulated in FXS patients (average age of 25) (Figure 7C), and additionally, the sAPPα product of ADAM10 activity was also increased in cells from FXS patients (Figure 7D). Finally, FMRP was IP from human control fibroblasts and the bound mRNAs were analyzed by RT-PCR, confirming that *APP* and *ADAM10* mRNAs are

Figure 3. FMRP Regulates the APP Processing Enzyme ADAM10

(A) ADAM10 expression is higher in *Fmr1* KO mice than in WT. Representative WB showing the ADAM10 protein levels in WT and KO cortices (black arrowheads: mature proteins and white arrowheads: prodomain containing proteins). The histograms show the quantification of ADAM10 and APP protein levels normalized to GAPDH levels expressed as ratio of the WT. The bars represent the SEM (*p < 0.05, **p < 0.01, Student's t test) (n = 3).

(B) ADAM10 expression is increased in synaptoneurosomes (Syn) from KO mice. Representative WB showing ADAM10, ADAM9, and ADAM17 expression levels in the WT and the KO mice (black arrowheads: mature protein and white arrowhead: immature protein). The histograms represent the quantification of protein levels normalized to GAPDH levels expressed as ratio of the WT. The bars represent the SEM (**p < 0.01, Student's t test) (n = 4).

(C) ADAM10 expression during development. ADAM10 protein levels were detected in WT and KO brain cortex extracts at P14, P21, P30, and P90. The GAPDH was used as normalizer. The bars represent the SEM (**p < 0.01, Student's t test) (n = 3).

(D) Immunofluorescence of ADAM10 in DIV14 cortical neurons. The left image shows representative dendritic fragments (>50 μm from cell body). The histograms represent protein levels quantified as the mean fluorescence intensity (Mean F.I.). The bars represent SEM (***p < 0.001, Student's t test) (n = 10 cells, five dendritic fragments [20 μm/cell]). The scale bar represents 5 μm.

(E) Surface ADAM10 is increased in *Fmr1* KO cortical neurons. Proteins were biotinylated and captured with streptavidin-Dynabeads; ADAM10 protein levels were analyzed by WB. The histograms show the quantification of the protein levels. The bars represent the SEM (*p < 0.05, **p < 0.01, one-sample t test) (n = 4).

(F) Detection of FMRP-associated mRNAs. The top panel shows a representative WB of FMRP-IP from brain extracts. Panels below show (RT-PCR to detect *App*, *Adam10*, *Adam9*, and *Adam17* mRNAs). Negative controls: dopamine receptor D2 (D_2DR) and (*Cyp46*) mRNAs. Positive control: α*CaMKII* mRNA. Lane 1, input (1/20); lane 2, αFMRP; and lane 3, control IgGs.

(G) Translational efficiency of *App* and *Adam10* mRNAs in WT and *Fmr1* KO cortices. The extracts were fractionated along a 10%–60% sucrose gradient. There were 12 fractions that were collected while reading the absorbance at 254 nm. The amount of *Adam10*, *App* and β-*actin* mRNAs in each fraction was quantified by RT-quantitative (q) PCR. A representative polysomal-mRNP profile is shown. Each fraction shows the quantification of *App* and *Adam10* mRNAs normalized to β-*actin* mRNA in the WT and *Fmr1* KO mice. The bars represent the SEM (*p < 0.05, **p < 0.01, Student's t test) (n = 4).

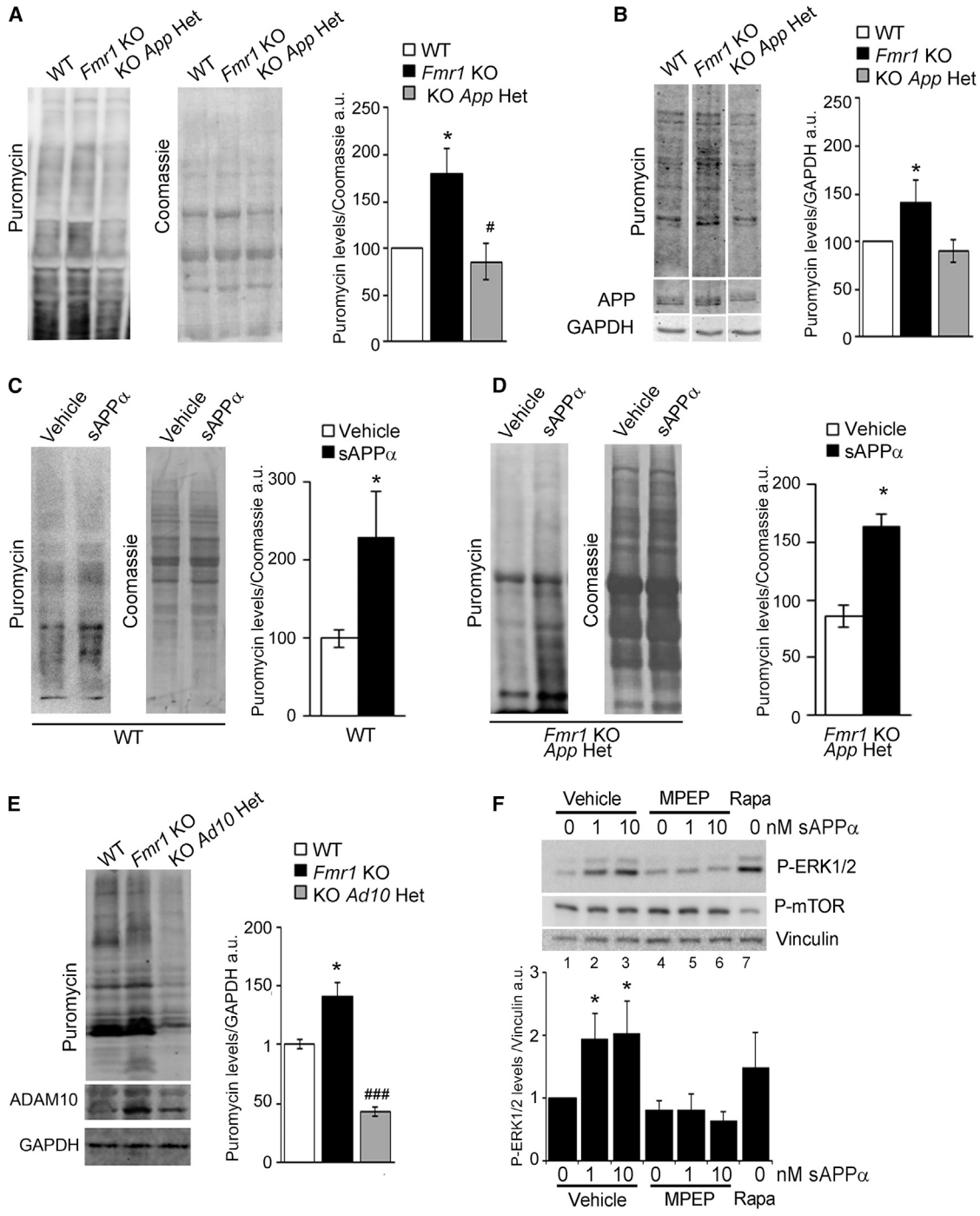

Figure 5. Exaggerated Protein Synthesis in *Fmr1* KO Depends on Excessive ADAM10 Activity and sAPPα Production

(A) Genetic reduction of APP in *Fmr1* KO mice ameliorates the excessive protein synthesis in cortical neurons. Representative WB showing incorporated puromycin in synaptoneurosomes. The histograms show the quantification of puromycin incorporation normalized to Coomassie. The bars represent the SEM (*$p < 0.05$ KO versus WT, $^{\#}$ $p < 0.05$ KO versus *Fmr1* KO/*App*^{Het}, one-sample t test) (Holm's correction) (n = 4 independent cultures).

(B) Protein synthesis in *Fmr1* KO/*App*^{Het} mice in synaptoneurosomes. Representative WB showing incorporated puromycin. The histogram shows a quantification of puromycin incorporation normalized to GAPDH. The bars represent the SEM. Kruskal-Wallis test followed by Dunn's post hoc test. (*$p < 0.05$) (n = 4 WT; n = 4 *Fmr1* KO; and n = 3 *Fmr1* KO/*App*^{Het}).

(C) sAPPα induces de novo protein synthesis. WT cortical neurons were treated with 1 nM sAPPα for 1 hr and analyzed as above. The bars represent the SEM (*$p < 0.05$, one-sample t test) (n = 3).

(D) sAPPα increases translation in the *Fmr1* KO/*App*^{Het}. Cortical neurons were treated with 1 nM sAPPα for 1 hr. The puromycin uptake was quantified by WB. The bars represent the SEM (*$p < 0.05$, one-sample t test) (n = 3).

(legend continued on next page)

associated to FMRP (Figure 7E). These findings demonstrate that APP and ADAM10 are also dysregulated in FXS human patients, and that ADAM10 dysregulation is possibly under developmental regulation in human patients.

DISCUSSION

Despite significant interest in the physiological functions of APP and its processed forms in the CNS, the mechanisms underlying APP developmental regulation and function(s) remain elusive. Dysregulation of APP and its metabolites, sAPPα and Aβ, have been observed in AD, autism, and Down syndrome (Glenner and Wong, 1984; Ray et al., 2011), suggesting that dysregulation of APP may have a key effect on neuronal pathologies marked by neurodegeneration and deficits in neurodevelopment.

Here, we show that sAPPα contributes to the three major hallmarks of FXS; namely, increased protein synthesis, aberrant spine morphology, and altered synaptic function and behavior. The expression of both APP and the α-secretase ADAM10 is controlled by FMRP during synaptogenesis (Figures 1, 3, and 8). Both proteins are upregulated in the absence of FMRP due to the lack of translational control on the respective mRNAs (Figures 3 and 8). Therefore, in FXS the unbalanced APP processing elicits excessive production of sAPPα (Figures 2 and 8).

The impairment in protein synthesis is linked to aberrant synaptic structure and plasticity in FXS (Bagni et al., 2012). We now show that the α-secretase activity is needed for the APP-mediated increase in protein synthesis, and administration of sAPPα causes FXS-like deficits, such as spine formation, maturation, and plasticity (Figures 4, 5, 6, and 8). Moreover, genetic reduction of APP or ADAM10 activity is sufficient to reduce protein synthesis in *Fmr1* KO neurons (Figure 6). Aberrant LTD in FXS mice is also rescued by the genetic downregulation of APP (Westmark et al., 2011), and ADAM10 activity has been related to LTD and spine morphology (Musardo et al., 2013; Prox et al., 2013), strongly suggesting that ADAM10-mediated APP cleavage is required in synaptic plasticity. Moreover, sAPPα is sufficient to rescue the anatomical, behavioral, and electrophysiological abnormalities of APP-deficient mice (Ring et al., 2007). Reduction of ADAM10 activity in vivo using a peptide inhibitor (Marcello et al., 2007) in juvenile *Fmr1* KO neurons restored normal sAPPα levels, prevented the exaggerated mGluR-LTD, and rescued behavioral deficits (Figures 6 and 8). In conclusion, excessive sAPPα, rather than full-length APP or Aβ, is involved in the synaptic pathology in FXS. Of relevance for the disease, we found that APP, ADAM10, and sAPPα levels were dysregulated in human samples (Figure 7).

Exaggerated mGluR1/5-dependent protein synthesis is one of the main features of FXS and is directly correlated to the increased mGluR-LTD (Bear et al., 2004). Throughout our studies, we have come full circle on a disease that over the last two decades has confronted us with an endless complexity. Lack of the translational repressor FMRP causes an increase of the mGluR1/5 signaling that promotes sAPPα release; in turn, sAPPα triggers ERK1/2 phosphorylation and sustains mGluR1/5 activation and protein synthesis (Figures 5 and 8). Blockade of the mGluR5 (Osterweil et al., 2010) or genetic reduction of APP reduces protein synthesis in the *Fmr1* KO (Figure 5).

Finally, our findings go beyond the role of APP and sAPPα in FXS: we provide new insights into the regulation of the non-amyloidogenic pathway and its role in synaptic function during a critical developmental window. APP protein expression and processing are developmentally controlled, as levels are higher in the second postnatal week during synaptogenesis and then decline when mature connections are completed (Moya et al., 1994). We demonstrate that FMRP regulates APP expression and processing only after the second postnatal week (Figures 1 and 2), concomitantly with the physiological decrease in APP. We propose that FMRP may intervene to avoid excessive APP and ADAM10 expression and sAPPα production during a critical period for synaptic stabilization and elimination (Yuste, 2013).

Our findings in humans (Figure 7) suggest that, similarly to the mouse model, the excess of APP and sAPPα triggers excessive protein synthesis, impaired synaptic LTD, leading to a detrimental effect on spine and brain function.

Considering the synaptic expression of APP, the neurotrophic function suggested for sAPPα (Hoe et al., 2012; Müller and Zheng, 2012) and its role in pruning (Olsen et al., 2014), the increased expression of sAPPα during synaptogenesis (Moya et al., 1994) could contribute to brain overgrowth and to defects in net spine pruning responsible for the abnormally high synaptic density observed in ASD (Tang et al., 2014). FXS is a neurodevelopmental disorder and patients with FXS have a high incidence of ASD. Children with severe autism and Fragile X express elevated levels of sAPPα (Erickson et al., 2014; Ray et al., 2011), consistent with the hypothesis for a sAPPα-mediated anabolic pathway in ASD (Lahiri et al., 2013). Therefore, it is tempting to hypothesize that alteration of the APP non-amyloidogenic pathway might be a shared feature of several neurodevelopmental disorders.

While the effect of sAPPα predominates, the excessive α-secretase activity upregulates CTFα and downregulates Aβ by competing with the β-secretase pathway or directly inhibiting BACE1 activity (Obregon et al., 2012). The APP CTFs can regulate signal transduction and apoptosis (Schettini et al., 2010) and we cannot exclude the possibility that their dysregulation also contributes to the FXS phenotypes. On the other hand, the amyloidogenic pathway is downregulated during synaptogenesis and we can therefore exclude a pathogenic effect of Aβ accumulation (Figure 2). On the contrary, since Aβ may stimulate neurotransmission (Morley et al., 2010), lower Aβ levels in FXS could exacerbate intellectual deficits.

(E) Basal protein synthesis in *Fmr1* KO/*Adam10*^{Het} synaptoneurosomes. Representative WB showing incorporated puromycin in synaptoneurosomes. The histograms show a quantification of puromycin incorporation normalized to GAPDH. The bars represent the SEM. Kruskal-Wallis test followed by Dunn's post hoc test. (*$p < 0.05$, ### $p < 0.001$ KO versus Fmr1 KO/*Adam10*^{Het}) (n = 4 WT; n = 4 *Fmr1* KO; and n = 3 *Fmr1* KO/*Adam10*^{Het}).

(F) sAPPα promotes mGluR1/5 signaling. Cortical neurons were treated for 1 hr with sAPPα with or without MPEP 50 μM or with Rapamycin 200 nM. Representative WB showing ERK 1/2 and mTOR phosphorylation levels. The histograms show a quantification of the protein levels normalized to Vinculin. The bars represent the SEM (*$p < 0.05$, one-way ANOVA followed by Dunnett's multiple comparisons test) (n = 5 independent cultures).

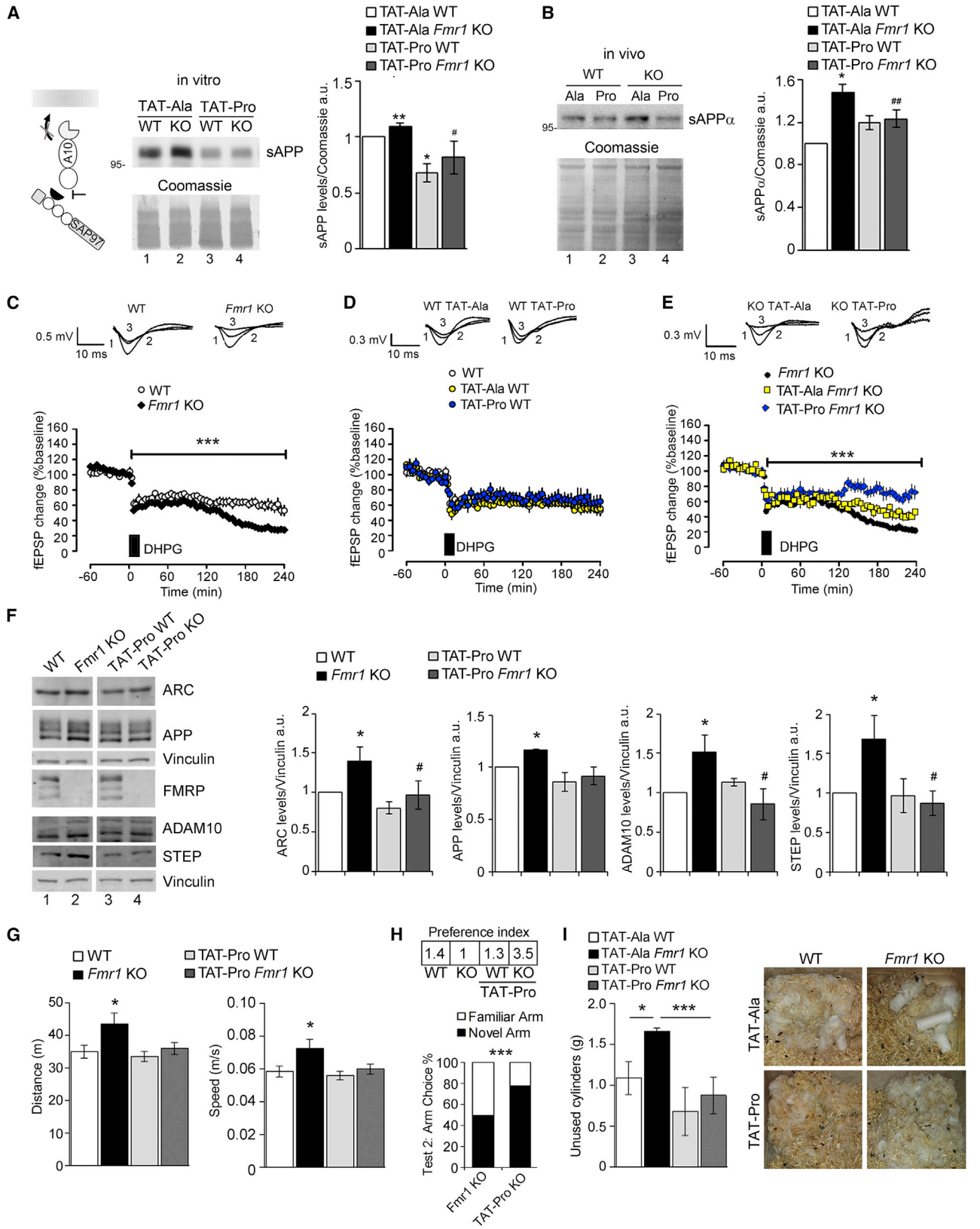

(legend on next page)

Increased APP levels are correlated with Aβ deposition in the brain; however, a mild increase in APP expression contributes to AD risk only at later ages (Brouwers et al., 2006). In old FXS mice, the equilibrium of the amyloidoigenic and non-amyloidoigenic pathways changes and there is a mild accumulation of Aβ (Figure 2). Further studies are required to address if the increase in APP levels observed in human FXS brains is sufficient to cause AD symptoms. Of note, higher incidence of dementia and cognitive deficits similar to those of AD was reported in elderly FXTAS patients with a decrease in FMRP expression (Seritan et al., 2008; Tassone et al., 2012).

Since the identification of the gene causing FXS in 1991, understanding and knowledge of the FMRP function(s) have increased (Bassell and Warren, 2008), but to date an effective therapy is still missing. Several therapeutic approaches for FXS have been explored and taken into clinical trials, however, several have been discontinued (https//:www.clinicaltrials.gov). Over the past few years, the FXS features observed in mice have been rescued through genetic reduction of single dysregulated genes (Bagni et al., 2012). The consequence of FMRP binding to several mRNAs in the brain (Pasciuto and Bagni, 2014b) is the impaired expression of a larger number of protein therefore identification of a key pathway, deregulated during a critical period of synaptic formation and brain connectivity, is therefore of utmost importance.

Although there are no pharmacological approaches to reduce APP expression, reduction of ADAM10 activity may provide an alternative approach for modulating sAPPα levels at synapses. We reduced ADAM10 synaptic localization and activity using the TAT-Pro peptide, a treatment previously shown to affect synaptic morphology and plasticity (Malinverno et al., 2010; Marcello et al., 2007). Treatment of juvenile *Fmr1* KO mice reduced APP α-cleavage, normalized enhanced LTD, and some behavioral deficits (Figures 6 and 8). Because of the high levels of sAPPα found in the blood of autistic patients (Ray et al., 2011) and in Fragile X children (Erickson et al., 2014), and the prevalence of autistic features in FXS, it is tempting to hypothesize that the activation of the ADAM10 pathway, leading to an excess of sAPPα production, is shared between patients with FXS and ASD. Finally, FXS symptoms suggest an early postnatal/childhood disruption of the brain wiring that may underlie ASD like features (La Fata et al., 2014; Romano et al., 2014). Based on our studies, we believe that the developmental period around synaptogenesis offers potentials for interventions to ameliorate some of the deficits observed in patients with FXS.

EXPERIMENTAL PROCEDURES

Human Samples

Patients' samples were received through clinical collaborators and co-authors of this study. Informed consent and ethical approval are available on site and at KU Leuven (Belgium).

Mice and Animal Care

Animal care was conducted conforming to institutional guidelines in compliance with international laws and policies (DL N116, GU, suppl 40, 18-2-1992; Belgian law KoninklijkBesluit (K.B.), 1993 and K.B, 2004; the European Community Council Directive 86/609, OJa L 358, 1, 1987; the National Institutes of Health Guide for the Care and Use of Laboratory Animals, US National Research Council, 1996). Studies were approved by the Institutional Ethical Board at the University of Leuven, Belgium. P7, P14, P21, P30, and P90 C57BL/6 WT and *Fmr1 KO* male mice (Bakker, 1994), APP KO (Li et al., 1996), and ADAM10^{Het} (Jorissen et al., 2010) were used in this study.

Animal Treatment

P19 and 20 mice received a single intraperitoneal injection of either TAT-Pro (2 or 3 nmol/g) or TAT-Ala peptide (2 or 3 nmol/g) diluted in sterile saline solution (Marcello et al., 2007). Animals were euthanized after 18 hr and the brains were rapidly removed. The TAT-Pro$^{709–729}$ ADAM10 inhibitory peptide (TAT-Pro) and TAT-Ala$^{709–729}$ADAM10 control peptide (TAT-Ala) were generated as previously described (Marcello et al., 2007).

Figure 6. Modulation of ADAM10 Activity Reduces Excessive sAPPα and Ameliorates LTD and Behavior in the *Fmr1* KO Mice

(A) Left scheme: TAT-Pro (in black) perturbs the ADAM10/SAP97 association and impairs ADAM10 (A10) localization at the cell surface. The treatment with TAT-Pro reduces sAPP release in neurons. The DIV15 cortical neurons were treated with TAT-Ala and TAT-Pro peptides (10 μM, 18 hr). The media was collected and sAPP levels were measured by WB (middle). The histograms show the quantification of sAPP normalized to Coomassie staining. The bars represent the SEM (*p < 0.05, **p < 0.01, versus TAT-Ala WT; # p < 0.05, TAT-Pro KO versus TAT-Ala KO, one-way ANOVA and Sidak's multiple comparisons test) (n = 3).

(B) ADAM10 activity can be modulated in vivo in the *Fmr1* KO. The juvenile mice (P21) received a single intraperitoneal injection of either a TAT-Pro (3 nmol/g) or TAT-Ala peptide (3 nmol/g). The effect on sAPPα release in the WT and KO brain cortices was monitored by WB after 18 hr. The histograms show the quantification of sAPPα protein levels normalized to Coomassie. The bars represent the SEM (*p < 0.05, TAT-Ala WT versus TAT-Ala KO; ## p < 0.01, TAT-Pro KO versus TAT-Ala KO, one-way ANOVA and Sidak's multiple comparisons test) (n = 5).

(C) *Fmr1* KO mice exhibit enhanced mGluR-LTD (n = 15 slices from nine mice/genotype).

(D) The mice (P18-P25) received a single intraperitoneal injection of either a Tat-Pro (2 nmol/g) or TAT-Ala peptide (2 nmol/g). TAT-Ala or TAT-Pro peptide does not impact LTD in the WT mice, whereas (E) TAT-Pro prevents mGluR-LTD in the *Fmr1*KO mice (F = 20, 75, p < 0.0002) (TAT-Pro n = 9 slices from six mice and TAT-Ala n = 8 slices from four mice). Solid bars indicate the duration of the bath application of DHPG (30 μM, 15 min). The representative traces (right) showing fEPSP before (1), 10 min after (2), and 240 min after (3) DHPG application. The stimulus artifact is blanked to ease interpretation. The data are shown as the means ± SEM. See also Figure S8.

(F) In vivo effects of TAT-Pro peptide treatment on protein expression in cortex. APP, ADAM10, ARC, and STEP protein levels were analyzed by WB. The bars represent the SEM (*p < 0.05, versus WT; #p < 0.05, TAT-Pro Ko versus KO, one-way ANOVA and Sidak's multiple comparisons test) (n = 5).

(G) Effect of the TAT-Pro peptide treatment on the performance of WT and *Fmr1* KO mice in the open field. Juvenile mice (P21) have been tested after 2 consecutive days of treatment with the peptide (2 nmol/g). Histograms represent the distance and the speed of the animals in the open field. (one-way ANOVA followed by Sidak's multiple comparisons test, and *p < 0.05). (n = 15 WT; n = 11 *Fmr1* KO; n = 14 TAT-Pro WT; and n = 17 TAT-Pro *Fmr1* KO).

(H) Effect of the peptide in the T-maze. The table shows the preference index for the novel arm in test 2 (1, no preference; >1, preference for the Novel Arm; and <1 preference for Familiar Arm. The histograms show the preference for the novel arm in the test 2 of the T-maze test (***p < 0.001, Chi square test) (n = 9 WT; n = 9 *Fmr1* KO; n = 9 TAT-Pro WT; and n = 12 TAT-Pro *Fmr1* KO).

(I) Effect of the TAT-Pro peptide treatment on the nest building performance of WT and *Fmr1* KO after 48 hr. The left histogram show the measure of the unused cotton cylinders (one-way ANOVA followed by Sidak's multiple comparisons test, *p < 0.05, and ***p < 0.001) (n = 8 WT; n = 8 *Fmr1* KO; n = 5 TAT-Pro WT; and n = 8 TAT-Pro *Fmr1* KO). The right images show representative examples of nest building in the tested conditions.

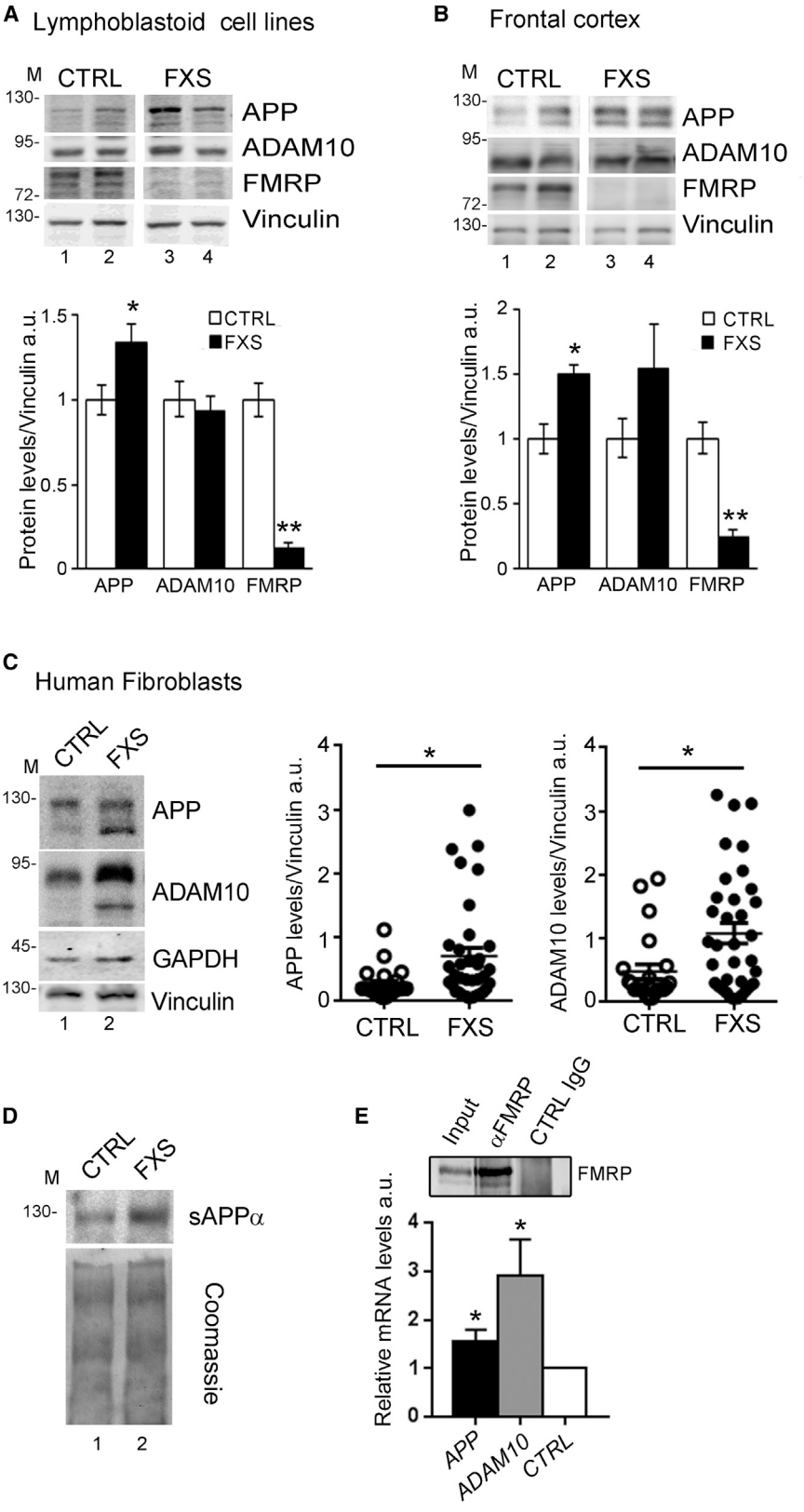

Figure 7. APP and ADAM10 Expression in Fragile X Patients

(A) APP and ADAM10 protein levels in human lymphoblastoid cells. Representative WB of APP, ADAM10, and FMRP protein levels in cell lines from healthy controls and FXS. The images belong to the same WB. The histograms show the quantification of APP, ADAM10, and FMRP normalized to Vinculin. The bars represent the SEM (*$p < 0.05$, **$p < 0.01$, and Student's t test) (n = 6 controls, 6 FXS).

(B) APP and ADAM10 levels in the cortex of FXS patients. The upper images show representative WB of APP and ADAM10 levels in the cortex of healthy controls and FXS (Table S1). The histograms show the quantification of APP, ADAM10, and FMRP normalized to Vinculin. The bars represent the SEM (*$p < 0.05$, **$p < 0.01$, Student's t test the prefrontal cortex) (n = 8 controls, 7 FXS).

(C) APP and ADAM10 levels in human fibroblasts. Shown are representative WBs detecting APP and ADAM10 levels in cells from healthy controls and FXS patients (left), and the quantification of APP (middle) and ADAM10 (right), normalized to GAPDH. The bars represent the SEM (*$p < 0.05$, Mann-Whitney test) (n = 7 controls, 8 FXS, at least three independent experiments shown in the graph).

(D) sAPPα in human FXS fibroblasts. Representative WB shows the levels of sAPPα in the media of control and FXS cells.

(E) IP of FMRP-associated mRNAs in human fibroblasts. RT-qPCR was used to detect *APP* and *ADAM10* mRNAs. The histograms represent the level of FMRP-bound mRNAs, the subtracted background was obtained by the IgGs. The average of the negative controls (CTRL): Vinculin (*VCL*), β-Glucuronidase (*GUSB*), *and* Hypoxanthineribosyltransferase (*HPRT*) mRNAs was set at 1 in each experiment (n = 3 controls, two independent experiments). The bars represent the SEM (*$p < 0.05$, one sample t test).

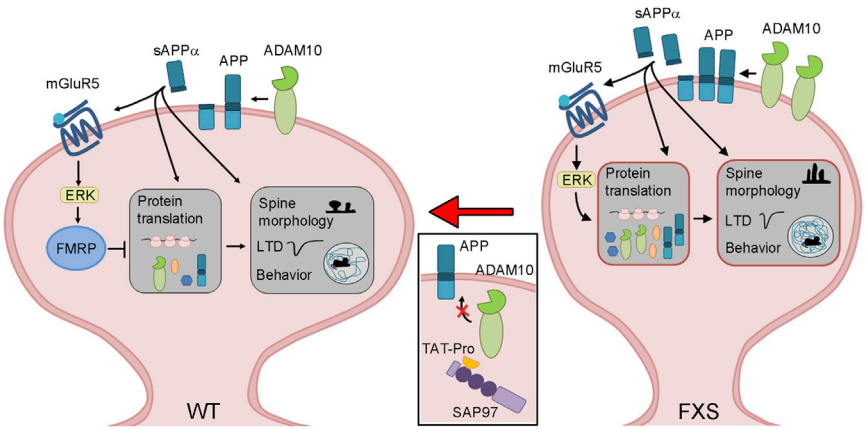

Figure 8. Restoring Synaptic Homeostasis in FXS

Left panel: in physiological conditions (WT) FMRP regulates the expression of several synaptic proteins downstream the mGluR1/5 signaling pathway. Among them it regulates the expression of APP and the α-secretase ADAM10. APP is cleaved by ADAM10 to generate sAPPα. sAPPα signals through the mGluR1/5 and activates the MAPK pathway, ultimately regulating protein translation affecting proper spine morphology, synaptic plasticity, and behavior. The right image shows that loss of FMRP (FXS) compromises the fine-tuned expression of a variety of synaptic proteins. This lack of translational control results in combined upregulation of APP and ADAM10 and accumulation of sAPPα. sAPPα triggers ERK1/2 phosphorylation and sustains mGluR1/5 activation and protein translation. Dysregulation of the APP-ADAM10 processing pathway leads to FXS deficits. Finally, reduction of ADAM10 trafficking/activity at synapses, using the TAT-Pro peptide, restores sAPPα levels, mGluR-LTD, protein expression, and behavioral deficits in FXS mice.

Neuronal Culture Preparation and Treatments

Mouse primary cortical neurons were prepared as previously described (De Rubeis et al., 2013). See Supplemental Information for details and treatments.

Human Fibroblasts and Lymphoblastoid Cell Lines

Fibroblasts from FXS subjects (n = 8, age range 12–37 years) were obtained from the University Hospital of Lausanne, while fibroblasts from healthy volunteers (n = 7, age range 15–42 years) were purchased from the Coriell Institute for Medical Research and from Lonza. Lymphoblastoid cell lines (CTR n = 6 and FXS n = 6) were obtained from University of California, Davis (UC Davis) (USA). See Supplemental Information for growth conditions.

Brain Protein Extracts

Brains lysates were prepared as previously described (Napoli et al., 2008). For details see the Supplemental Information. For enriched membrane proteins, 1% sodium deoxycholate was added and the extracts were incubated for 30 min on ice and centrifuged. For total protein analysis, the brains or cells were homogenized in Laemmli buffer as previously described (Napoli et al., 2008).

Synaptoneurosomes

Synaptoneurosomes were prepared as previously described (Pilo Boyl et al., 2007). For details see the Supplemental Information.

WB

Standard methodologies were used. Antibodies list and usage is described in the Supplemental Information.

SUnSET

A protein synthesis assay was performed using the SUnSET method (Schmidt et al., 2009). For details see the Supplemental Information.

DNA Constructs

The pEGFP plasmid used is commercially available (Clontech). The pLentiLox3.7 (pLL3.7) vector containing the shRNA against APP (targeting nt 538-556 of APP Genbank:X59379.1) has been previously described (Hoe et al., 2009); it is specific for both mouse and rat APP and was kindly provided by Dr. Daniel Pak (Georgetown University Medical Center).

Transfection

Neurons were transfected at 8 days in culture using the calcium phosphate method as previously described (De Rubeis et al., 2013). Neurons were fixed 6 days later with 4% paraformaldehyde/sucrose EDTA magnesium PFA/SEM (4% PFA, 0.12 M sucrose, 3 mM EGTA, and 2 mM MgCl2 in PBS). Confocal images were acquired and analyzed as described in the Supplemental Information.

Immunofluorescence

For experimental details and antibodies list and usage see the Supplemental Information.

IP and RT-PCR

IP protocol was modified from Napoli et al. (2008). For details see the Supplemental Information.

Polysome-mRNPs Analysis

Polysome-mRNPs have been isolated as previously described (Zalfa et al., 2007). For details see the Supplemental Information.

RT-Quantitative PCR Using the SYBRGreen Method

Real-Time PCR was performed using the SYBRGreen mix and a Light Cycler 480 (Roche).

Biotinylation Assay

Biotinylation of cell surface proteins was performed as previously described (Hiltunen et al., 2006). For details see the Supplemental Information.

Aβ 40-42 ELISA

The brains were solubilized in guanidine hydrochloride, and Aβ was detected using a sandwich ELISA assay according to the manufacturer's specifications (WACO).

Brain Fractionation

See the Supplemental Information and Figure S2.

Electrophysiology

The mGluR mediated LTD was induced as previously described (Tambuyzer et al., 2013). For details see the Supplemental Information.

Behavioral Tests

All behavioral experiments were performed with P24 and 25 male mice and blind to the genotype and treatment. For experimental details see the Supplemental Information.

Statistics

Comparisons between the two groups were performed using one-sample or two-sample two-tailed Student's t tests. One-way ANOVA followed by a

post hoc Holm's, Bonferroni's, or Sidak's multiple comparisons test was performed. Distributions were analyzed using the Pearson's chi-square (χ^2) test. Comparisons between the cumulative probability plots were performed using a two-sample Kolmogorov-Smirnov (K-S) test. Significance was denoted as $p < 0.05$. Bars represent the SEM. Electrophysiological data were analyzed using repeated-measures ANOVA.

SUPPLEMENTAL INFORMATION

Supplemental Information includes Supplemental Experimental Procedures, eight figures, and one table, and can be found with this article online at http://dx.doi.org/10.1016/j.neuron.2015.06.032.

ACKNOWLEDGMENTS

This work was supported by grants from Stichting Alzheimer Onderzoek - Fondation Recherche Maladie Alzheimer (SAO-FMA), Vlaams Instituut voor Biotechnologie (VIB), KU Leuven (Opening the Future), European Research Projects on Neurodevelopmental Disorders NEURON ERA-NET, Associazione Italiana Sindrome X Fragile and Compagnia San Paolo to C.B., a European Research Council Grant ERC-2010-AG_268675 to B.D.S.; a Methusalem grant of the KU Leuven/Flemish Government to B.D.S. and C.D. B.D.S. is supported by the Bax-Vanluffelen Chair for Alzheimer's Disease. C.B. and B.D.S. are supported by "Opening the Future" of the Leuven Universiteit Fonds (LUF). E.P. has been awarded a Fonds Wetenschappelijke Onderzoek (FWO) aspirant fellowship. T.A. and D.B. are supported by an interdisciplinary research grant from KU Leuven Geconcerteerde Onderzoeksactie (GOA) 12/008. U.C.M. was supported by grants from Deutsche Forschungsgemeinschaft (DFG) (MU 1457/8-1; 1457/9-1). We are extremely grateful to Silvia De Rubeis, Daniele Di Marino, Elena Marcello, and Tilmann Achsel for sharing preliminary data, scientific discussions, and critical reading of the manuscript. We thank Nathalie Leysen, Jonathan Royaert, and Karin Jonckers for their excellent technical help. We are very grateful to Eef Lemmens for her outstanding administrative support. We are thankful to Sebastian Munck, coordinator of Light Microscopy and Imaging Network (LiMoNe, KU Leuven) for his precious advice. The Nikon microscope used in this study was acquired through a Hercules Type 1 AKUL/09/037 to Wim Annaert that we would like to thank also for providing the ADAM10 antibody. Inframouse (KU Leuven and VIB infrastructures were fundamental for the mouse work described here.

Received: November 9, 2013
Revised: April 23, 2015
Accepted: June 23, 2015
Published: July 15, 2015

REFERENCES

Amour, A., Knight, C.G., Webster, A., Slocombe, P.M., Stephens, P.E., Knäuper, V., Docherty, A.J., and Murphy, G. (2000). The in vitro activity of ADAM-10 is inhibited by TIMP-1 and TIMP-3. FEBS Lett. *473*, 275–279.

Bagni, C., Tassone, F., Neri, G., and Hagerman, R. (2012). Fragile X syndrome: causes, diagnosis, mechanisms, and therapeutics. J. Clin. Invest. *122*, 4314–4322.

Bakker, C.; The Dutch-Belgian Fragile X Consortium (1994). Fmr1 knockout mice: a model to study fragile X mental retardation. Cell *78*, 23–33.

Bassell, G.J., and Warren, S.T. (2008). Fragile X syndrome: loss of local mRNA regulation alters synaptic development and function. Neuron *60*, 201–214.

Bear, M.F., Huber, K.M., and Warren, S.T. (2004). The mGluR theory of fragile X mental retardation. Trends Neurosci. *27*, 370–377.

Bell, K.F., Zheng, L., Fahrenholz, F., and Cuello, A.C. (2008). ADAM-10 over-expression increases cortical synaptogenesis. Neurobiol. Aging *29*, 554–565.

Bittner, T., Fuhrmann, M., Burgold, S., Jung, C.K., Volbracht, C., Steiner, H., Mitteregger, G., Kretzschmar, H.A., Haass, C., and Herms, J. (2009). Gamma-secretase inhibition reduces spine density in vivo via an amyloid precursor protein-dependent pathway. J. Neurosci. *29*, 10405–10409.

Brouwers, N., Sleegers, K., Engelborghs, S., Bogaerts, V., Serneels, S., Kamali, K., Corsmit, E., De Leenheir, E., Martin, J.J., De Deyn, P.P., et al. (2006). Genetic risk and transcriptional variability of amyloid precursor protein in Alzheimer's disease. Brain *129*, 2984–2991.

Comery, T.A., Harris, J.B., Willems, P.J., Oostra, B.A., Irwin, S.A., Weiler, I.J., and Greenough, W.T. (1997). Abnormal dendritic spines in fragile X knockout mice: maturation and pruning deficits. Proc. Natl. Acad. Sci. USA *94*, 5401–5404.

Darnell, J.C., and Klann, E. (2013). The translation of translational control by FMRP: therapeutic targets for FXS. Nat. Neurosci. *16*, 1530–1536.

De Rubeis, S., Pasciuto, E., Li, K.W., Fernández, E., Di Marino, D., Buzzi, A., Ostroff, L.E., Klann, E., Zwartkruis, F.J., Komiyama, N.H., et al. (2013). CYFIP1 coordinates mRNA translation and cytoskeleton remodeling to ensure proper dendritic spine formation. Neuron *79*, 1169–1182.

Erickson, C.A., Ray, B., Maloney, B., Wink, L.K., Bowers, K., Schaefer, T.L., McDougle, C.J., Sokol, D.K., and Lahiri, D.K. (2014). Impact of acamprosate on plasma amyloid-β precursor protein in youth: a pilot analysis in fragile X syndrome-associated and idiopathic autism spectrum disorder suggests a pharmacodynamic protein marker. J. Psychiatr. Res. *59*, 220–228.

Galli, T., McPherson, P.S., and De Camilli, P. (1996). The V0 sector of the V-ATPase, synaptobrevin, and synaptophysin are associated on synaptic vesicles in a Triton X-100-resistant, freeze-thawing sensitive, complex. J. Biol. Chem. *271*, 2193–2198.

Genheden, M., Kenney, J.W., Johnston, H.E., Manousopoulou, A., Garbis, S.D., and Proud, C.G. (2015). BDNF stimulation of protein synthesis in cortical neurons requires the MAP kinase-interacting kinase MNK1. J. Neurosci. *35*, 972–984.

Glenner, G.G., and Wong, C.W. (1984). Alzheimer's disease and Down's syndrome: sharing of a unique cerebrovascular amyloid fibril protein. Biochem. Biophys. Res. Commun. *122*, 1131–1135.

Grant, S.G. (2012). Synaptopathies: diseases of the synaptome. Curr. Opin. Neurobiol. *22*, 522–529.

Harris, K.M., Jensen, F.E., and Tsao, B. (1992). Three-dimensional structure of dendritic spines and synapses in rat hippocampus (CA1) at postnatal day 15 and adult ages: implications for the maturation of synaptic physiology and long-term potentiation. J. Neurosci. *12*, 2685–2705.

Hick, M., Herrmann, U., Weyer, S.W., Mallm, J.P., Tschäpe, J.A., Borgers, M., Mercken, M., Roth, F.C., Draguhn, A., Slomianka, L., et al. (2015). Acute function of secreted amyloid precursor protein fragment APPsα in synaptic plasticity. Acta Neuropathol. *129*, 21–37.

Hiltunen, M., Lu, A., Thomas, A.V., Romano, D.M., Kim, M., Jones, P.B., Xie, Z., Kounnas, M.Z., Wagner, S.L., Berezovska, O., et al. (2006). Ubiquilin 1 modulates amyloid precursor protein trafficking and Abeta secretion. J. Biol. Chem. *281*, 32240–32253.

Hinton, V.J., Brown, W.T., Wisniewski, K., and Rudelli, R.D. (1991). Analysis of neocortex in three males with the fragile X syndrome. Am. J. Med. Genet. *41*, 289–294.

Hoe, H.S., Lee, K.J., Carney, R.S., Lee, J., Markova, A., Lee, J.Y., Howell, B.W., Hyman, B.T., Pak, D.T., Bu, G., and Rebeck, G.W. (2009). Interaction of reelin with amyloid precursor protein promotes neurite outgrowth. J. Neurosci. *29*, 7459–7473.

Hoe, H.S., Lee, H.K., and Pak, D.T. (2012). The upside of APP at synapses. CNS Neurosci. Ther. *18*, 47–56.

Huber, K.M., Gallagher, S.M., Warren, S.T., and Bear, M.F. (2002). Altered synaptic plasticity in a mouse model of fragile X mental retardation. Proc. Natl. Acad. Sci. USA *99*, 7746–7750.

Irwin, S.A., Patel, B., Idupulapati, M., Harris, J.B., Crisostomo, R.A., Larsen, B.P., Kooy, F., Willems, P.J., Cras, P., Kozlowski, P.B., et al. (2001). Abnormal dendritic spine characteristics in the temporal and visual cortices of patients with fragile-X syndrome: a quantitative examination. Am. J. Med. Genet. *98*, 161–167.

Jacquemont, S., Hagerman, R.J., Hagerman, P.J., and Leehey, M.A. (2007). Fragile-X syndrome and fragile X-associated tremor/ataxia syndrome: two faces of FMR1. Lancet Neurol. *6*, 45–55.

Jorissen, E., Prox, J., Bernreuther, C., Weber, S., Schwanbeck, R., Serneels, L., Snellinx, A., Craessaerts, K., Thathiah, A., Tesseur, I., et al. (2010). The disintegrin/metalloproteinase ADAM10 is essential for the establishment of the brain cortex. J. Neurosci. *30*, 4833–4844.

Kang, J., Lemaire, H.G., Unterbeck, A., Salbaum, J.M., Masters, C.L., Grzeschik, K.H., Multhaup, G., Beyreuther, K., and Müller-Hill, B. (1987). The precursor of Alzheimer's disease amyloid A4 protein resembles a cell-surface receptor. Nature *325*, 733–736.

Karran, E., Mercken, M., and De Strooper, B. (2011). The amyloid cascade hypothesis for Alzheimer's disease: an appraisal for the development of therapeutics. Nat. Rev. Drug Discov. *10*, 698–712.

Kuhn, P.H., Wang, H., Dislich, B., Colombo, A., Zeitschel, U., Ellwart, J.W., Kremmer, E., Rossner, S., and Lichtenthaler, S.F. (2010). ADAM10 is the physiologically relevant, constitutive alpha-secretase of the amyloid precursor protein in primary neurons. EMBO J. *29*, 3020–3032.

La Fata, G., Gärtner, A., Domínguez-Iturza, N., Dresselaers, T., Dawitz, J., Poorthuis, R.B., Averna, M., Himmelreich, U., Meredith, R.M., Achsel, T., et al. (2014). FMRP regulates multipolar to bipolar transition affecting neuronal migration and cortical circuitry. Nat. Neurosci. *17*, 1693–1700.

Lahiri, D.K., Sokol, D.K., Erickson, C., Ray, B., Ho, C.Y., and Maloney, B. (2013). Autism as early neurodevelopmental disorder: evidence for an sAPPα-mediated anabolic pathway. Front. Cell. Neurosci. *7*, 94.

Lee, E.K., Kim, H.H., Kuwano, Y., Abdelmohsen, K., Srikantan, S., Subaran, S.S., Gleichmann, M., Mughal, M.R., Martindale, J.L., Yang, X., et al. (2010a). hnRNP C promotes APP translation by competing with FMRP for APP mRNA recruitment to P bodies. Nat. Struct. Mol. Biol. *17*, 732–739.

Lee, K.J., Moussa, C.E., Lee, Y., Sung, Y., Howell, B.W., Turner, R.S., Pak, D.T., and Hoe, H.S. (2010b). Beta amyloid-independent role of amyloid precursor protein in generation and maintenance of dendritic spines. Neuroscience *169*, 344–356.

Li, Z.W., Stark, G., Götz, J., Rülicke, T., Gschwind, M., Huber, G., Müller, U., and Weissmann, C. (1996). Generation of mice with a 200-kb amyloid precursor protein gene deletion by Cre recombinase-mediated site-specific recombination in embryonic stem cells. Proc. Natl. Acad. Sci. USA *93*, 6158–6162.

Lichtenthaler, S.F. (2011). α-secretase in Alzheimer's disease: molecular identity, regulation and therapeutic potential. J. Neurochem. *116*, 10–21.

Lozano, R., Rosero, C.A., and Hagerman, R.J. (2014). Fragile X spectrum disorders. Intractable Rare Dis. Res. *3*, 134–146.

Ma, X.M., and Blenis, J. (2009). Molecular mechanisms of mTOR-mediated translational control. Nat. Rev. Mol. Cell Biol. *10*, 307–318.

Malinverno, M., Carta, M., Epis, R., Marcello, E., Verpelli, C., Cattabeni, F., Sala, C., Mulle, C., Di Luca, M., and Gardoni, F. (2010). Synaptic localization and activity of ADAM10 regulate excitatory synapses through N-cadherin cleavage. J. Neurosci. *30*, 16343–16355.

Marcello, E., Gardoni, F., Mauceri, D., Romorini, S., Jeromin, A., Epis, R., Borroni, B., Cattabeni, F., Sala, C., Padovani, A., and Di Luca, M. (2007). Synapse-associated protein-97 mediates alpha-secretase ADAM10 trafficking and promotes its activity. J. Neurosci. *27*, 1682–1691.

Milosch, N., Tanriöver, G., Kundu, A., Rami, A., François, J.C., Baumkötter, F., Weyer, S.W., Samanta, A., Jäschke, A., Brod, F., et al. (2014). Holo-APP and G-protein-mediated signaling are required for sAPPα-induced activation of the Akt survival pathway. Cell Death Dis. *5*, e1391.

Morley, J.E., Farr, S.A., Banks, W.A., Johnson, S.N., Yamada, K.A., and Xu, L. (2010). A physiological role for amyloid-beta protein:enhancement of learning and memory. J. Alzheimers Dis. *19*, 441–449.

Moya, K.L., Benowitz, L.I., Schneider, G.E., and Allinquant, B. (1994). The amyloid precursor protein is developmentally regulated and correlated with synaptogenesis. Dev. Biol. *161*, 597–603.

Müller, U.C., and Zheng, H. (2012). Physiological functions of APP family proteins. Cold Spring Harb. Perspect. Med. *2*, a006288.

Musardo, S., Marcello, E., Gardoni, F., and Di Luca, M. (2013). ADAM10 in synaptic physiology and pathology. Neurodegener. Dis. *13*, 72–74.

Napoli, I., Mercaldo, V., Boyl, P.P., Eleuteri, B., Zalfa, F., De Rubeis, S., Di Marino, D., Mohr, E., Massimi, M., Falconi, M., et al. (2008). The fragile X syndrome protein represses activity-dependent translation through CYFIP1, a new 4E-BP. Cell *134*, 1042–1054.

Nosyreva, E.D., and Huber, K.M. (2005). Developmental switch in synaptic mechanisms of hippocampal metabotropic glutamate receptor-dependent long-term depression. J. Neurosci. *25*, 2992–3001.

Obregon, D., Hou, H., Deng, J., Giunta, B., Tian, J., Darlington, D., Shahaduzzaman, M., Zhu, Y., Mori, T., Mattson, M.P., and Tan, J. (2012). Soluble amyloid precursor protein-α modulates β-secretase activity and amyloid-β generation. Nat. Commun. *3*, 777.

Olsen, O., Kallop, D.Y., McLaughlin, T., Huntwork-Rodriguez, S., Wu, Z., Duggan, C.D., Simon, D.J., Lu, Y., Easley-Neal, C., Takeda, K., et al. (2014). Genetic analysis reveals that amyloid precursor protein and death receptor 6 function in the same pathway to control axonal pruning independent of β-secretase. J. Neurosci. *34*, 6438–6447.

Osterweil, E.K., Krueger, D.D., Reinhold, K., and Bear, M.F. (2010). Hypersensitivity to mGluR5 and ERK1/2 leads to excessive protein synthesis in the hippocampus of a mouse model of fragile X syndrome. J. Neurosci. *30*, 15616–15627.

Panja, D., Kenney, J.W., D'Andrea, L., Zalfa, F., Vedeler, A., Wibrand, K., Fukunaga, R., Bagni, C., Proud, C.G., and Bramham, C.R. (2014). Two-stage translational control of dentate gyrus LTP consolidation is mediated by sustained BDNF-TrkB signaling to MNK. Cell Rep. *9*, 1430–1445.

Pasciuto, E., and Bagni, C. (2014a). SnapShot: FMRP interacting proteins. Cell *159*, 218–218.e1.

Pasciuto, E., and Bagni, C. (2014b). SnapShot: FMRP mRNA targets and diseases. Cell *158*, 1446.

Pilo Boyl, P., Di Nardo, A., Mulle, C., Sassoè-Pognetto, M., Panzanelli, P., Mele, A., Kneussel, M., Costantini, V., Perlas, E., Massimi, M., et al. (2007). Profilin2 contributes to synaptic vesicle exocytosis, neuronal excitability, and novelty-seeking behavior. EMBO J. *26*, 2991–3002.

Prox, J., Bernreuther, C., Altmeppen, H., Grendel, J., Glatzel, M., D'Hooge, R., Stroobants, S., Ahmed, T., Balschun, D., Willem, M., et al. (2013). Postnatal disruption of the disintegrin/metalloproteinase ADAM10 in brain causes epileptic seizures, learning deficits, altered spine morphology, and defective synaptic functions. J. Neurosci. *33*, 12915–12928, 12928a.

Rajendran, L., and Annaert, W. (2012). Membrane trafficking pathways in Alzheimer's disease. Traffic *13*, 759–770.

Ray, B., Long, J.M., Sokol, D.K., and Lahiri, D.K. (2011). Increased secreted amyloid precursor protein-α (sAPPα) in severe autism: proposal of a specific, anabolic pathway and putative biomarker. PLoS ONE *6*, e20405.

Reinhard, C., Borgers, M., David, G., and De Strooper, B. (2013). Soluble amyloid-β precursor protein binds its cell surface receptor in a cooperative fashion with glypican and syndecan proteoglycans. J. Cell Sci. *126*, 4856–4861.

Rice, H.C., Young-Pearse, T.L., and Selkoe, D.J. (2013). Systematic evaluation of candidate ligands regulating ectodomain shedding of amyloid precursor protein. Biochemistry *52*, 3264–3277.

Ring, S., Weyer, S.W., Kilian, S.B., Waldron, E., Pietrzik, C.U., Filippov, M.A., Herms, J., Buchholz, C., Eckman, C.B., Korte, M., et al. (2007). The secreted beta-amyloid precursor protein ectodomain APPs alpha is sufficient to rescue the anatomical, behavioral, and electrophysiological abnormalities of APP-deficient mice. J. Neurosci. *27*, 7817–7826.

Roch, J.M., Masliah, E., Roch-Levecq, A.C., Sundsmo, M.P., Otero, D.A., Veinbergs, I., and Saitoh, T. (1994). Increase of synaptic density and memory retention by a peptide representing the trophic domain of the amyloid beta/A4 protein precursor. Proc. Natl. Acad. Sci. USA *91*, 7450–7454.

Romano, D., Nicolau, M., Quintin, E.M., Mazaika, P.K., Lightbody, A.A., Cody Hazlett, H., Piven, J., Carlsson, G., and Reiss, A.L. (2014). Topological

methods reveal high and low functioning neuro-phenotypes within fragile X syndrome. Hum. Brain Mapp. *35*, 4904–4915.

Sala, C., and Segal, M. (2014). Dendritic spines: the locus of structural and functional plasticity. Physiol. Rev. *94*, 141–188.

Santos, A.R., Kanellopoulos, A.K., and Bagni, C. (2014). Learning and behavioral deficits associated with the absence of the fragile X mental retardation protein: what a fly and mouse model can teach us. Learn. Mem. *21*, 543–555.

Schettini, G., Govoni, S., Racchi, M., and Rodriguez, G. (2010). Phosphorylation of APP-CTF-AICD domains and interaction with adaptor proteins: signal transduction and/or transcriptional role–relevance for Alzheimer pathology. J. Neurochem. *115*, 1299–1308.

Schmidt, E.K., Clavarino, G., Ceppi, M., and Pierre, P. (2009). SUnSET, a nonradioactive method to monitor protein synthesis. Nat. Methods *6*, 275–277.

Selkoe, D.J. (2002). Alzheimer's disease is a synaptic failure. Science *298*, 789–791.

Seritan, A.L., Nguyen, D.V., Farias, S.T., Hinton, L., Grigsby, J., Bourgeois, J.A., and Hagerman, R.J. (2008). Dementia in fragile X-associated tremor/ataxia syndrome (FXTAS): comparison with Alzheimer's disease. Am. J. Med. Genet. Neuropsychiatr. Genet. *147B*, 1138–1144.

Tambuyzer, T., Ahmed, T., Taylor, C.J., Berckmans, D., Balschun, D., and Aerts, J.M. (2013). System identification of mGluR-dependent long-term depression. Neural Comput. *25*, 650–670.

Tang, G., Gudsnuk, K., Kuo, S.H., Cotrina, M.L., Rosoklija, G., Sosunov, A., Sonders, M.S., Kanter, E., Castagna, C., Yamamoto, A., et al. (2014). Loss of mTOR-dependent macroautophagy causes autistic-like synaptic pruning deficits. Neuron *83*, 1131–1143.

Tassone, F., Greco, C.M., Hunsaker, M.R., Seritan, A.L., Berman, R.F., Gane, L.W., Jacquemont, S., Basuta, K., Jin, L.W., Hagerman, P.J., and Hagerman, R.J. (2012). Neuropathological, clinical and molecular pathology in female fragile X premutation carriers with and without FXTAS. Genes Brain Behav. *11*, 577–585.

Tyan, S.H., Shih, A.Y., Walsh, J.J., Maruyama, H., Sarsoza, F., Ku, L., Eggert, S., Hof, P.R., Koo, E.H., and Dickstein, D.L. (2012). Amyloid precursor protein (APP) regulates synaptic structure and function. Mol. Cell. Neurosci. *51*, 43–52.

Udagawa, T., Farny, N.G., Jakovcevski, M., Kaphzan, H., Alarcon, J.M., Anilkumar, S., Ivshina, M., Hurt, J.A., Nagaoka, K., Nalavadi, V.C., et al. (2013). Genetic and acute CPEB1 depletion ameliorate fragile X pathophysiology. Nat. Med. *19*, 1473–1477.

Westmark, C.J., and Malter, J.S. (2007). FMRP mediates mGluR5-dependent translation of amyloid precursor protein. PLoS Biol. *5*, e52.

Westmark, C.J., Westmark, P.R., O'Riordan, K.J., Ray, B.C., Hervey, C.M., Salamat, M.S., Abozeid, S.H., Stein, K.M., Stodola, L.A., Tranfaglia, M., et al. (2011). Reversal of fragile X phenotypes by manipulation of AβPP/Aβ levels in Fmr1KO mice. PLoS ONE *6*, e26549.

Yuste, R. (2013). Electrical compartmentalization in dendritic spines. Annu. Rev. Neurosci. *36*, 429–449.

Zalfa, F., Eleuteri, B., Dickson, K.S., Mercaldo, V., De Rubeis, S., di Penta, A., Tabolacci, E., Chiurazzi, P., Neri, G., Grant, S.G., and Bagni, C. (2007). A new function for the fragile X mental retardation protein in regulation of PSD-95 mRNA stability. Nat. Neurosci. *10*, 578–587.